Back-Barrier Sediment and Hydrodynamic Processes: Insights from Rodanthe, NC

by

Christopher J. Cornette

July, 2016

Co-Directors of Thesis: D. Reide Corbett and J.P. Walsh

Major Department: Geological Sciences

Abstract

Barrier islands are found around the world, and their geomorphic evolution is related to ocean and estuarine processes. Processes including sediment mobilization and shoreline evolution on both the ocean and estuarine side of barrier islands, control long-term evolution through many short-term (days) events (e.g., hurricanes, nor'easters). The Outer Banks of North Carolina are bounded by the Atlantic Ocean and the Albemarle and Pamlico Sound Estuarine System, the second largest estuary in the U.S. Back-barrier environments in the system are extensive with over 1500 km of estuarine shoreline in Dare County (McVerry, 2012). The back-barrier coast of Rodanthe, a small town on the Outer Banks, consists of an undulating shoreline, adjacent to a broad (~4 km) shallow shoal (<2 m) widely covered with submerged aquatic vegetation (SAV). Shoreline and volumetric change rates, bathymetry, surface sediment grain properties, and hydrodynamic conditions were measured to evaluate sediment processes, SAV coverage and change over time. Understanding these back-barrier sediment processes is important for navigation, shoreline, and ecosystem management.

Shoreline change rates (SCR) were evaluated using aerial photographs from five time steps (i.e., 1949, 1974, 2007, 2012, 2015). The average long-term SCR across the study region was -0.41 m y^{-1}, but there was much variability. Data show the southern shoreline dominated by

erosion and marsh loss with an increase in sediment banks and modification. Single-beam bathymetric confirmed the presence of a broad (~4 km) back-barrier shoal. Surface sediment grab samples displayed a dominance of fine sands with modest variation in grain size across the region and very low mud percent and organic content. Bathymetric change of the emergency navigational channel showed large deposition, and the timing suggests the importance of storm-related transport (e.g. Hurricanes Isabel, Ophelia, Irene). Calculated bed shear stresses based on the measured waves and currents indicate that bed shear stress during storms can exceed threshold of motion conditions (i.e., 0.18 N/m^2) for the mean basin grain size (199 μm). Aerial photography revealed the area was largely covered by SAV. Occurrence of SAV over 10 years showed little variation with consistent coverage. An optimal depth range of SAV (0.5-2.2 m) was determined based on bathymetric mapping.

Three conclusions were derived from data: (1) Erosion and shoreline hardening are both important shoreline change process along on the back-barrier. High shoreline erosion rates and marsh shoreline loss lead to an increase in sediment banks or anthropogenically modified shorelines. (2) Critical shear stresses of motion are exceeded episodically with fresh breezes or stronger winds (>10 m s^{-1}), and ferry channel bathymetry suggest considerable sediment transport and deposition during high-wind events (e.g., hurricanes). The dominant back-barrier shoal sediments were clean, medium sands (i.e., low mud %, low loss on ignition). The low mud percent and low loss on ignition are likely maintained by regular wave reworking. (3) SAV in the study area has been persistent through time at water depths between 0.5-2.2 m. This depth range is consistent with other SAV studies and is attributable to water-level and light limitations.

Back-Barrier Sediment and Hydrodynamic Processes: Insights from Rodanthe, NC

A Thesis

Presented to the Faculty of the Department of Geological Sciences

East Carolina University

In Partial Fulfillment of the Requirements for the Degree

Masters of Science in Geology

By

Christopher J. Cornette

July, 2016

Back-Barrier Sediment and Hydrodynamic Processes: Insights from Rodanthe, NC

by

Christopher J. Cornette

APPROVED BY:

DIRECTOR OF THESIS: _____
D. Reide Corbett, PhD

CO-DIRECTOR: _____
J. P. Walsh, PhD

COMMITTEE MEMBER: _____
David Mallinson, PhD

COMMITTEE MEMBER: _____
Michael Piehler, PhD

CHAIR OF THE DEPARTMENT
OF GEOLOGICAL SCIENCES: _____
Stephen Culver, PhD

DEAN OF THE
GRADUATE SCHOOL: _____
Paul Gemperline, PhD

Acknowledgements

This thesis could not have been accomplished without the help, support and academic encouragement of many people. I would first like to thank my advisers Dr. Walsh and Dr. Corbett for their continued support. Through their guidance I have grown academically and professionally. I have learned and experienced much through them and my research. I would also like to thank my committee members Dr. Mallinson and Dr. Piehler for their guidance.

Many people have helped with data collection and processing methods. I owe my deepest gratitude for ArcGIS knowledge to Keith Garmire. Data collection and processing was greatly aided by the help of Kieth Garmire, Émeric Bourineau, David Hawkins, Ian Conery, Luke Stevens, Nick Kelly, Ryan Gibbons and Brian Querry among others.

Great thanks are due to John Woods who helped setup and maintain remote class technologies. I am also appreciative of all of my ECU professors, especially those who worked with me through remote learning to facilitate my research in the Outer Banks.

I am grateful for the community at the UNC Coastal Studies Institute. Through the facility I was provided access to plentiful research support. Through the faculty and staff I was invited into a family that encouraged my intellectual growth and fostered my curiosity of the coastal environment.

Financial support was provided in part for this project by the North Carolina Department of Transportation.

Table of Contents

List of Tables

List of Figures

1.0 INTRODUCTION

Barrier islands are found around the world, and they are important ecologically and economically (Stutz and Pilkey, 2001; Feagin et al., 2010). Their natural geomorphic evolution is related to ocean and estuarine processes including sediment mobilization and shoreline evolution on both the ocean and estuarine side of the land (Riggs et al., 1995; Timmons et al., 2010; Riggs et al., 2011). Change occurs related to many short-term (days) events (e.g., hurricanes, nor'easters) and longer-term evolution over years to decades as geomorphic responses. In modern barrier environments, anthropogenic impacts add another facet to barrier evolution (Riggs et al., 2009; Timmons et al., 2010). Further understanding of the complex interplay of modern processes and anthropogenic forcings in the back-barrier environment is necessary for predicting barrier island evolution.

This research occurs along the Outer Banks (OBX) of North Carolina, which is a series of dynamic barrier landforms, and its evolution has been influenced by both natural and artificial processes (Culver et al., 2006; Riggs et al., 2009; Currin and Deaton, 2010). Landward of the OBX is the Albemarle Pamlico Sound Estuarine System, the second largest estuary in the U.S. Back-barrier environments in the system are extensive with over 1500 km of estuarine shoreline in Dare County (McVerry, 2012). The town of Rodanthe, NC is a small unincorporated town on Hatteras Island that is bound to the north by Pea Island National Wildlife Refuge and to the south by the towns of Waves and Salvo. This study aims to better understand the interface of the back-barrier and sound in and near the town of Rodanthe, NC.

Like other barriers, the OBX is made up of a patchwork of habitats that make up the coastal landforms of barrier islands (Fig. 1), and these areas may show rapid change in response to winds, waves and currents. In addition, tides drive water flow through inlets and influence

flooding of the beach and back-barrier habitats. The underlying geology is the platform upon which this system operates, and it may influence the dynamics such as inducing erosional hot spots (Riggs et al., 1995; McNinch, 2004; Miselis and McNinch, 2006). Human influence on barrier islands (e.g. shoreline hardening, nourishment, navigational channels) further complicates barrier dynamics and influences long-term barrier evolution (Culver et al., 2006; Riggs et al., 2009). Barrier islands are diverse in their processes and interactions between these processes and the natural and man-made environments are complicated.

This study aims to improve our understanding of the natural and human processes acting on the modern back-barrier system of Hatteras Island. Through observations and measurements of shoreline change, waves, currents, and sediment characteristics, the relationships between physical processes, anthropogenic activities and the changing shallow-water habitat were evaluated. Specific objectives of this project were to: 1) measure spatial and temporal patterns of shoreline change using aerial imagery and RTK-GPS and quantify shoreline erosion as a potential source of sediment into the study region; 2) characterize the sediments and evaluate their relation to physical forces (e.g., waves, currents) that act to move and deposit material in and beyond the study area; and 3) evaluate bathymetric dynamics and the spatial extent and persistence of SAV in the study region as both are important for management characteristics.

2.0 BACKGROUND

2.1 Geologic History

The morphology and stratigraphy of the modern OBX barrier system has an important relation to the Last Glacial Maximum, ~18,000 years BP (Mallinson et al., 2005; Clark et al., 2009). Since that time, paleo-river valleys of Pamlico Creek and the Tar and Neuse rivers were flooded as sea level rose leading to the unique estuarine morphology of today (Mallinson et al., 2010). Pamlico Creek (modern Pamlico Sound) was a body of water separated from the eastern barrier islands and the ocean by a high-elevation peninsular region known as the Hatteras Flats Interstream Divide. However, at approximately 5,000 years BP the interstream divide was inundated by rising seas forming what is the present day Pamlico Sound (Riggs and Ames, 2003; Mallinson et al., 2005; Culver et al., 2007; Zarimba et al., in press).

Exchange between the Pamlico Sound and the Atlantic occurs at several inlets through the islands. Historically, inlets have opened and closed at various locations throughout the region with major inlets existing for several centuries (Fig. 2) (Riggs, 1995; Riggs, 2009; Mallinson et al., 2010). New Inlet is the closest inlet to the study area in modern history. Based on historical accounts, it opened in the 1700s and separated Bodie Island and Hatteras Island, but began to shoal after the opening of Oregon Inlet in 1846. New Inlet closed completely in 1922 (Stick, 1958; Fisher, 1967; Riggs et al., 2009). It briefly reopened in 1933 to 1945, and in 2011 Hurricane Irene breached the island forming “New” New Inlet (aka Irene Inlet) (Clinch et al., 2012; Mulligan et al., 2014). The two modern inlets that bound Hatteras Island are Oregon Inlet to the north of the study area and Hatteras Inlet to the southwest. Hatteras inlet opened with Oregon Inlet in 1846 due to a strong hurricane (Mallinson et al., 2010).

Ground penetrating radar surveys, coring and optically stimulated luminescence dating were used by Mallinson et al. (2010) to detail the great extent of paleo-inlet channels across the Outer Banks. It has been demonstrated that portions of Hatteras Flats are composed of relict flood tidal deltas that were deposited during a period of high storm frequency and active open marine exchange between the Pamlico Sound and Atlantic Ocean approximately 1000 calendar years BP, during the Medieval Climate Anomaly (Fig. 3) (Culver et al., 2006; Mallinson et al., 2011; Peek et al., 2013). Peake et al. (2013) address the origin of sand bars that establish bathymetric relief on the subtidal back-barrier platform. The platform of Hatteras Flats provides a stage for modern processes.

2.2 Pea Island and Rodanthe Back-Barrier

The area around Rodanthe has a diversity of back-barrier environments adjacent to Pamlico Sound with shoreline types that include marshes, sediment banks, and human modified areas. The boundaries of this study extended slightly north and south of Rodanthe to encompass a broader perspective on processes (Fig. 4). To the north of Rodanthe is the Pea Island National Wildlife Refuge, a federally protected and managed area with expansive back-barrier marshes and channels with little development. To the south lie the towns of Waves, Salvo, Avon and eventually Buxton near Cape Hatteras. In the center of Rodanthe is an emergency ferry terminal that serves as a means of transportation when the road (i.e., Hwy 12) is impassable due to island overwash or other closures. The area adjacent to the ferry terminal is marsh that extends further soundward than the nearby back-barrier shoreline. Hatteras Flats is a subtidal shoal that extends ~4 km landward (into the sound) of the back-barrier shoreline (Riggs et al., 1995; Riggs et al.,

2009). The Flats are continuous from Pea Island through Ocracoke Island but have variable sound-ward extent (Riggs et al., 2009).

2.3 Hydrodynamics

The astronomical tidal range is low in the APES due to its shallow nature and restricted inlet flow (Benninger and Wells, 1993; Luettich et al., 2000; Reed et al., 2008). Predicted tides for Rodanthe have a range of ~30 cm (NOAA Station 8653215, Rodanthe, NC). Currents related to the tides are minimal; currents in the APES are enhanced by wind-forced conditions (Luettich et al., 2000; Dillard, 2008).

The large Pamlico Sound fetch, wind strength, and duration dictate the magnitude of waves and wind currents (Wells and Kim, 1989; Luettich et al., 2002; Dillard, 2008; Mulligan et al., 2014). Drag forces due to surface friction between wind and water creates waves, which form orbital motion that propagates downward in the water column. When orbital velocities are strong enough and the water column is shallow enough, waves can create a stress on the sediment bed (τ_w). Using measured values of significant wave height (H_s, the mean of the highest one third of measured waves) and peak wave period (T_p, the wave period with the highest energy), τ_w (calculated) can exceed the threshold of sediment motion (Whitehouse et al., 2001; Dillard, 2008). Winds are seasonal in the Pamlico Sound and predominantly S-SW in summer and N-NE in winter (Benninger and Wells, 1993; Leuttich, 2002; Reynolds-Flemming and Leuttich, 2004; Whipple, Luettich, and Seim, 2006), aligning with the length of greatest fetch. Sustained winds and storm winds are capable of inundating the back-barrier which can remobilize or deposit new sediments beyond the shoreline (e.g. Hurricane Irene, 2011; Clinch et al., 2012; Hardin et al, 2012; Mulligan et al., 2014).

Erosion of marine sediments occurs when either τ_w (wave shear stress) or τ_c (current shear stress), or a combination of the two, exceed τ_{cr} (critical bed shear stress), considering sediment type and cohesiveness (Whitehouse et al., 2001; Ziervogul, 2003; Grabowski et al., 2011). Critical bed shear stress is governed by a variety of factors and varies substantially with sediment type, organic content, etc. The inclusion of >5% mud-size grains increases cohesion, increasing τ_{cr} significantly (Ziervogul, 2003; Grabowski et al., 2011). Sediment bed properties (such as τ_{cr}) can be calculated theoretically in regions with low fine-grained percentages due to the expected lesser influence of cohesion (Ziervogul, 2003). Past studies have shown that winds are a significant driver of sediment resuspension in the Pamlico Sound, and the associated waves and/or wind can be measured to predict sediment resuspension frequency (Booth, 2000; Dillard, 2008).

2.4 Shoreline Processes

Back-barrier shoreline change is a process that controls barrier island width as well as the geologic evolution of the island (Smith et al., 2008; Timmons et al., 2010; Conery, 2014). Net change of the estuarine shoreline is dictated by natural sediment supply processes such as ocean overwash and inlet formation, as well as back-barrier attributes including sediment composition and elevation (Smith et al., 2008; Cowart et al., 2010). Storm events are also a significant process in back-barrier shoreline change due to resuspension and redistribution of sediments (Phillips, 1999; Gittman et al., 2014). Some research has shown that marshes can act as a natural barrier against erosion and potentially work better than human-emplaced hard structures (Gittman et al., 2014).

Estuarine shoreline change has been measured and calculated using several methods. A common method employs heads-up digitization of georectified aerial photography or satellite images (Fig. 5) (Jackson et al., 2012; Eulie et al., 2014). Eulie et al. (2014) measured short-term (sub-annual) shoreline change using balloon aerial photography. With several years of shoreline change, transect based approaches can be used to calculate point-value shoreline change rates (SCR) across a region (Jackson et al., 2012). Changes in back-barrier shoreline type influences SCRs, which in turn may impact back-barrier sediment processes (Gittman et al., 2014; Cowart et al., 2010; Jackson et al., 2002).

2.5 Submerged Aquatic Vegetation

Research has shown that SAV has a significant impact on local sediment deposition through wave and current attenuation (Koch, 2001; Chen et al., 2007). However, surface sediment grain size readily dictates SAV colonization (Koch et al., 2001; Swerida, 2013). Several models have been used to qualitatively evaluate SAV shoot attenuation of currents and waves (Peterson et al., 2004; Chen et al., 2007; Zeller et al., 2014). However, research by Luhar et al. (2010) concluded that wave orbital velocity within SAV beds is only marginally attenuated when compared with the more dramatic attenuation of unidirectional flow (i.e., currents).

Recent work by Palinkas and Koch (2012) assessed sediment trends (e.g. accumulation, grain size, sediment supply) across several SAV habitats in the Chesapeake Bay and their results yielded conceptual models of SAV based on sediment processes and properties (Fig. 6). Sandy sediments, low organic content and moderate (3-9 mm y^{-1}) sediment accretion rates characterized persistent SAV beds (Palinkas and Koch, 2012). They hypothesize sediment sources may have significant impact on SAV habitat stability, where fine-grained sediments prevent colonization

and sands are easily colonized. Based on their conceptual model a change in shoreline type may negatively affect SAV habitats due to an alteration of sediment supply (Adair et al., 1994; Palinkas and Koch, 2012).

Studies have shown that SAV attenuates waves and currents enough to possibly increase fine-grained mud and organic matter deposition, which leads to a build-up of carbon in SAV sediments (Kennedy et al., 2010; Fourqurean et al., 2012; Greiner et al., 2013). Sustained SAV presence and environmental influence in this way can act to enhance carbon burial (Greiner et al., 2013). However, other research has hypothesized the increase of organic content in sediments promotes SAV populations with a high leaf to stem length ratio, making these areas more susceptible to erosion (Wicks et al., 2009). Regardless, the broad scope of past research suggests a complex relationship between SAV and sediment processes that will vary on different spatial scales coincident with depositional regimes.

3.0 METHODS

3.1 Shoreline Data Collection and Analysis

In this study shoreline change rates were evaluated over several time scales (e.g., seasonal, decadal) to help evaluate processes influencing change (e.g., Cowart et al., 2010; Geis and Bendell, 2010; Jackson, 2010). Shoreline data was obtained for 1949 (from Outer Banks History Center), 1974 (from National Park Service, Manteo, NC), 2007 (NC DCM, 2007), and 2012 (NC DCM, 2012). Also, a 2015 shoreline was mapped for the study area using a combination of RTK-GPS and aerial imagery. The RTK-GPS survey was conducted by walking the shoreline along the wet-dry line for sediment bank shore type and on the scarp for marsh shorelines (Eulie et al., 2013; Eulie, 2014; Strand, 2015). Hard structures were measured by walking on (seawall) or basinward (rip-rap) and then later checked based on aerial images for georeference. Areas inaccessible by foot within the Pea Island National Wildlife Refuge shoreline were defined by fish-eye-corrected Go Pro aerial imagery (Fig. 5), collected in October 2015. The 2015 images were georectified by second-order polynomial with greater than 10 control points (Cowart et al., 2010). The shoreline was digitized in a heads-up fashion (on a computer screen) using the vegetation boundary or wet-dry line in sediment banks (Cowart et al., 2010; Geis and Bendell, 2010). Wind-induced water level changes at the time of photography may add error due to shoreline location appearance.

Shoreline change rates (SCR) were evaluated with the Analyzing Moving Boundaries Using R (AMBUR) package that measures boundary change across a series of transects (Jackson et al, 2010, 2012; Eulie et al, 2014). Baselines were created with the buffer tool in ArcMap at a distance of 100 m from the nearest shoreline before casting transects. Transect spacing distance was set at 50 m using the AMBUR package. Transects were filtered by AMBUR and manually

to reduce error by excess shoreline capture and to ensure shore normality. Long-term (1949 – 2015) and short-term (i.e., 1949-1974, 1974-2007, 2007-2012, 2012 – 2015) SCRs were calculated.

Aerial images were used to classify shoreline polylines into one of three shoreline types: marsh, sediment bank, or modified (e.g., seawall, rip-rap) following methods outlined by Geis and Bendell, 2010. Length and percentage of each shoreline type was calculated from the shoreline polylines using ArcGIS (Version 10.2). To help synthesize the data, shoreline data are reported for four discrete sub-regions. The sub-regions were classified by the modern shoreline type with the highest presence (e.g. marsh, modified, sediment bank).

3.2 Volumetric Change Analysis

Volumetric change rates (VCR) of shorelines show a sediment flux from shoreline erosion that is delivered to the adjacent basin (Biribo and Woodroffe, 2013; Zhou et al., 2014; Davies-Vollum and West, 2015; Hawkins, 2015). This study used three methods for VCR calculations to provide a range of shoreline volume change. Method 1 calculated the VCR by multiplying a scarp height, SCR and shoreline length. Scarp heights were determined for each shoreline region using RTK-measured elevations taken at the top and bottom of scarps. Relief data from at least five scarps were averaged to calculate the mean scarp height for each region. Method 2 calculated shoreline length relative to an ArcGIS-defined baseline in an effort to account for potential loss in tortuosity of the shoreline. Method 3 used the mean scarp height and a polygon of lost shorezone area change between two time steps (i.e., 1949 and 2015) to calculate estimate volume loss. Error from Method 3 was based on the shoreline mapping error and scarp height error.

3.3 Bathymetry

Bathymetry was measured in the study area with a Sonarmite Echo Sounder synced with a Trimble TSC5 (handheld) and RTK-GPS SPS882 (receiver). The echosounder was mounted on the gunnel of a small vessel, and data was collected along track lines across the study region (Fig. 4). Echosounder data were obtained during days with low winds to reduce error associated with boat heave, pitch and roll. Depth values were determined relative to the NAD83 datum. All data were combined in ArcGIS and the Kriging tool was used to interpolate between data points to create a seamless bathymetry.

Bathymetric (XYZ) data for the emergency ferry channel also was obtained from the NC DOT for various surveys during the 1995-2014 time period. Data were imported into ArcMap and krigged to produce a raster surface (Fig. 7). Raster surfaces from older bathymetric surveys were subtracted from newer surveys using the Raster Calculator tool in ArcGIS to estimate depth change between time steps. Areas of non-overlap were not analyzed. Volume change between data years was calculated by summing the product of the cell area and vertical change for all analyzed cells (calculated in ArcMap).

3.4 Sediment Characterization and SAV Coverage

To understand sediment and SAV coverage, samples and observations were made on a grid across the study region (Fig. 4). The first collection retrieved 45 samples (Fig. 4). Subsequent sampling retrieved a smaller subset of the original samples, at 14 sites across the study area. A bulk sample of surface sediment (100 to 300 g) was collected using a grab at each site. It was placed in a whirl-pack bag and stored until processed.

Because of very limited mud in the area, all samples were analyzed for grain size using a dry sieve method. Sediments were homogenized, and a 50 to 100 g subsample was dried at 105 °C for 24 hrs. Subsamples were then dry-sieved via Ro-Tap with sieves ranging from 4 to -2 ϕ (1/2 ϕ increments) to measure mud to very fine gravel (Open File Report 00-358, http://pubs.usgs.gov/of/2000/of00358/text/chapter1.htm,http://woodshole.er.usgs.gov/openfile/of2005-1001/htmldocs/videos/dry_sieve/dry_sieve.htm). Grain-size statistics were calculated using the GRADISTAT-2008 program (Blott and Pye, 2001).

Loss on ignition (LOI) was measured on all samples; it is often used to calculate percent organic content (Dean, 1974; Heiri et al., 2001). When organic matter is heated past 500 °C, it is oxidized to ash and carbon dioxide. The percent change in mass of a dry sample pre and post-ignition at 500 °C is a measurable removal of organic matter (Heiri et al., 2001). A 5 to 10 g subsample was initially dried at 105 °C for 24 hours. Then, the mass loss was measured after combustion at 550 °C for 8 hours (Dean, 1974; Heiri, 2001; Strand, 2015).

SAV coverage data was assessed visually in the field during the first sediment sample collection. Presence (i.e., present or absent) and qualitative density (i.e., no SAV, patchy, moderate or extensive) was evaluated at all sites. Also, SAV coverage was mapped using imagery from Google Earth Pro. Images from 2004, 2005, 2009, 2010, and 2014 were saved, clipped and georeferenced in ArcGIS. All images used were from the July-October when SAV coverage was likely to be well developed. SAV boundaries were heads-up digitized to evaluate distribution across the study area. These data were later converted into polygons to measure recurrence (Orth et al, 2014). An error depth (2.5 m) was defined where increased water depth prevented identification of the SAV-sediment boundary in the 2014 image. A 22 x 22 grid of

points was used to extract depth and SAV data across the study area. The values at each point were plotted to evaluate the relationship between SAV and depth.

3.5 Wave and Current Measurements

Several hydrodynamic instruments were used to measure waves and currents. A Nortek Vector current meter and an OBS-3+ turbidity sensor were mounted on a constructed deployment platform. Both instruments were set to measure 25 cm above bed at 8 Hz for 2048 samples (~4 minutes) at one hour intervals. The instrument platform was deployed just outside of the Rodanthe emergency ferry channel (Fig. 4). The platform was deployed for ~1 month.

Data from the deployments were processed with QuickWave software to determine wave height and period (Dillard, 2008). The law of the wall equation was used to calculate bed shear stress from the current velocity data (Soulsby, 1983; Soulsby and Humphery, 1990; Ziervogul, 2003):

$$u(z) = \frac{u_*}{K} \cdot \ln\left(\frac{z}{z_0}\right) \qquad \text{Eq. 1}$$

where z is a measured height above bed (i.e., 25 cm in the deployment); u_* is the shear velocity which is related to the bed stress; K is the Von Karman constant equal to 0.41 (unitless), and z_0 is the roughness length, the height above bed in which velocity becomes zero (Soulsby, 1983; Ziervogul, 2003). Roughness length was assumed to be 0.006 m based on data from Soulsby (1983) and presence of ripples (observed on instrument deployment) on sandy bottom. Solving equation 1 for u_* for any measured velocity 25 cm above bed with a rippled sandy bottom gives:

$$u_* = u(25\ cm) \cdot 0.097 \qquad \text{Eq. 2}$$

where u and u_* are defined above. Measured currents were also processed using the turbulent kinetic energy method to estimate the bed shear stress (Kim et al., 2000; Pope et al., 2006).

4.0 RESULTS

4.1 Shoreline Change

With 50-m spacing, SCR was measured along 181 transects for each time step. Change values showed prominent erosion across the region, with only a few areas showing accretion. The accretion zones were in areas of modified shoreline (i.e. bulkhead, rip rap) that extended basinward of historic shoreline. The mean SCR for each time step was negative except for 2007-2012 (0.01 ± 0.32 m y^{-1}), which was within the error of no measurable change (Table 1).

The "Modern" shoreline change was determined by comparing the RTK-GPS mapped shoreline in 2015 with the 2012 digitized shoreline (Fig. 9). SCR ranged from -10 to +5 m y^{-1}. Thirty-two of the 181 transects displayed accretion. Of those accretion points, only 12 exceeded the measurement error (± 0.56 m y^{-1}). The accretion spots were associated with areas of sediment banks or modified shoreline where new hard structures (e.g., rip rap, bulkhead) had been emplaced.

Long-term shoreline change was measured using the offset of the 1949 and 2015 aerial photos. Mean shoreline change using all transects was -27.9 ± 2.1 m with a mean change rate of -0.41 ± 0.03 m y^{-1} (Fig. 9). The highest accretion areas were sediment banks with <0.50 m y^{-1}. The highest erosion rates (~2.0 m y^{-1}) were found in southern marsh regions of Pea Island National Wildlife Refuge and a separate area in Rodanthe made up of sediment banks that were anthropogenically modified by 2015. Marshes in the central portion of the study and areas far to the north and south yielded the lowest shoreline change rates.

Shoreline type varied significantly across the study area. Data were analyzed by discrete subregion to help synthesize the shoreline attributes (Fig. 10; note R# indicates the region number). Region 1 (R1) had marsh as the major shoreline type (>90%) across all time steps.

Variation in shore type was greater than R1 in Region 2 (R2) with a decrease in marsh and increase in sediment bank through time with the exception of the 2012 shoreline. In 2015, one portion of the shoreline in R2 was classified as modified because of a new revetment. Marsh shoreline represented less than 50% during all observation periods. Region 3 (R3) exceeded 70% marsh through all time steps. A minor increase in the modified and sediment bank shore types was noted in 2007 through 2015. Region 4 (R4) experienced a significant change from being dominated by marsh and sediment bank in 2007 to almost 85% modified in 2015. Region 5 (R5) maintained >60% marsh since 1949, but has lost sediment bank shoreline to modification in recent years.

4.1.1 Volumetric Change Rates

To evaluate volume change, scarp measurements were made at several areas in each region, and data were averaged to provide a representative value for the region. The greatest mean scarp was in R3 (i.e., the ferry terminal marsh) at 0.55 m. Mean scarp values for R1, R2 and R5 were 0.23, 0.45 and 0.47 m, respectively. No scarps were measured in R4 due to high amount of shoreline modification.

Volume change rates calculated for each region varied greatly by method, but all indicated a significant release of sediments to the sound. Using Method 1, i.e., the SCR-based method, calculated subregion values ranged from -240 to -800 m^3/y. For the Method 2, estimates were between -150 and -240 m^3/y, and Method 3 gave values that ranged from -160 to -320 m^3/y. Regions 2 and 3 had the highest volume loss regardless of the method. Total volume change rates across the study area also varied by method and were -1900 m^3/y, -760 m^3/y, -970 m^3/y respectively.

4.2 Bathymetry

The single beam bathymetry surveys confirmed the presence of a broad (>3 km wide), shallow (<1.5 m depth) shoal region, i.e., the "Flats", along the back-barrier shore (Fig. 4). Two, especially shallow, shore-parallel areas (<0.5 m) are also noticeable near the western edge of the Flats. Two channel-like depressions penetrate at least 2 km into the back-barrier shoal system. The northern channel connects to the soundward (western) extent of the emergency ferry channel and has apparently been dredged in the past for navigational purposes by the United States Army Corps of Engineers (USACE) (Army Corps of Engineers, Reports: 01 Nov 2012; 26 Nov 2012; 15 Jul 2013). There is no record of USACE dredging in the southern channel.

Changes in bathymetry through time for the emergency ferry channel show periods of large losses (dredging) and gains of material (i.e., deposition events). Volumetric change calculated between the measurement time intervals was variable (Fig. 11). Periods of loss appear to correlate with dredging operations preceding measurements in the years 1998, 2001, and 2011-2012 (Department of the Army/Corps of Engineers, 2012, 2011, 2010, 1998, 1997). Three periods of channel shoaling, or bathymetric gain, occurred prior to the mapping in 2004, 2005 and 2011. Change preceding the 2005 step is an increase of 53,000 m^3. Losses (negative changes) in channel sediment volumes range from -5,000 to -50,000 m^3; the highest loss volume was estimated between the 2012 and 2013 channel mappings.

4.3 Meteorological Data and Hydrodynamics

Meteorological data retrieved for three hurricanes (i.e., Isabel, September 18, 2003, Ophelia, September 14, 2005 and Irene, August 27, 2011) reveal high sustained winds and gusts of tropical storms (Fig. 12). Maximum recorded sustained winds for Isabel were southerly and

exceeded 20 m s^{-1} before station outages (Fig. 12). Sustained winds during Ophelia and Irene exceeded 25 m s^{-1}at nearby sites (Diamond Shoals data buoy and Oregon Inlet Marina, respectively), with gusts exceeding 35 m s^{-1} (Fig. 12). Winds were generally from east during Ophelia and Irene and then shifted to the southwest after the systems passed. Each of these storms impacted the study region just days prior to bathymetric surveys of the emergency ferry channel (USACE, Reports: Sep. 18, 2005; Aug. 31, 2011).

Vector and OBS data from an August-September deployment measured waves and currents, and calculations show bed shear stresses exceeded τ_{cr} during two periods of high winds (Fig. 13). Theoretical τ_{crit} of fine sands across the basin is estimated to be 0.18 N/m^2 (http://pubs.usgs.gov/sir/2008/5093) based on the basin sediment mean grain size (see below). The first resuspension event (Sep. 13, 2015) was brief with wave heights reaching ~0.5 m, while the second event (Sep. 24, 2015) had smaller waves (H_s <0.1 m) but the bed stress exceeded the threshold for motion for an extended period of time. The sustained wind direction was largely different between events. The wave event (i.e. Fig. 13, blue box) showed sustained SW winds and the current event (i.e. Fig. 13, green box) showed sustained N-NE winds.

4.4 Sediment Character

A total of 46 surface samples were collected in June, 2015 (Fig. 4), and data show a dominance of sand in the area. Mud content was always <6% (Fig. 14), and mean grain sizes were from 122 to 284 μm. For all samples, an average mean grain size of 199 μm (fine sand) was determined. Values for d_{50}, varied from very fine sand (>64 μm) to medium sand (<450 μm). Values for d_{10} always were in the fine to very find sand range, ranging from 67 to 160 μm, and d_{50} values ranged from 101 to 259 μm (very fine to medium sand) (Fig. 14). The maximum d_{90}

value was 431 μm, and the lowest was 172 μm. Based on the average mean grain size (199 μm, a fine sand), the theoretical critical bed shear stress is ~0.18 N/m^2 (USGS, 2008-5093).

A total of 16 sediment samples were collected in December, 2015, and 14 of those were from sites previously sampled. Average mean grain size was 208 μm (fine sand) for these samples. Values for December d50 deviated from June samples slightly (decrease of >-10 and increase of <42 μm) (Fig. 14). A comparison using two-tailed t-test of the June and December resampled subset showed no statistical difference.

Sediment samples collected in both June and December had very low LOI. Only one sample exceeded 1% LOI (Fig. 14). December sediments appeared to have slightly higher values for LOI (Table 2), although none exceeded 1%. Scarp samples taken within the study area displayed much higher LOI, between 5 and 26%.

4.5 Submerged Aquatic Vegetation

Mapping of SAV using historical aerial photography showed widespread coverage in the study area (Fig. 8). SAV was most prominent in the eastern portion of the study area. No SAV was noted in the western (deeper) parts of the study area. Extent of SAV varied little with time (Fig. 15). Area of coverage varied from 25 to 31 km^2 (Table 3). The greatest variation occurs at along the seaward (deepest) boundary where SAV was more difficult to discern due to depth. A visible habitat break occurs in all time steps at the shallow areas ~4 km west of the shoreline. Also, a sharp edge in SAV habitat was commonly seen nearshore. Several areas of ephemeral SAV habitats were mapped in the north. Based on the frequency of cover mapping (Fig. 15, lower right), SAV covered 45% of the study area during at least one time step, and 29% of the area was covered during all five time steps.

Analysis of bathymetry and SAV occurrence along a grid of points across the area showed SAV was distributed in a discrete depth band (Fig. 16). SAV occurrence ranged from 0.4 to 2.7 m depth. SAV occurrence for all five observations (i.e., persistent coverage) was limited to a depth range of 0.5 to 2.2 m. The mode for the occurrence of SAV (both >0 and all observations) was 1.3 to 1.4 m.

5.0 DISCUSSION

5.1 Shoreline Loss and Transformation

Shoreline change rates measured in this study agree with previous studies along the Outer Banks estuarine shoreline (Dolan et al., 1993; Smith et al., 2008; Eulie et al., 2013; Conery, 2014). Areas of moderate to high erosion rates have been attributed to limited back-barrier sediment supply and high wave energy in large fetch areas (Riggs and Ames, 2003; Riggs et al., 2009; Eulie et al., 2014). SCRs for each time step show widespread erosion throughout the study area, except during the 2007-2012 period (Fig. 9; Table 1). The limited amount of erosion during the 2007-2012 time step is surprising as Hurricane Irene impacted the region with high winds and storm surge (Fig. 12) (Mulligan et al., 2014). Other research on storms has shown their predominantly erosive effects on back-barrier and estuarine shorelines (Riggs et al., 2009; Timmons et al., 2010; McNinch et al., 2012; Eulie et al., 2013). The areas of accretion between 2007 and 2012 were in areas of increased bulkheads and revetments. The shoreline modification (and lateral, basinward accretion) shows the impact of anthropogenic response to hurricane erosion recovery.

Estuarine marsh has been shown to have significantly lower rates of shoreline erosion compared to sediment banks, so a loss of marsh and transition to sediment bank ultimately increases susceptibility of high rates of erosion (Cowart et al., 2011; Shepard et al., 2011; Pinsky et al., 2013; Gittman et al., 2014). Shoreline regions with persistent marsh presence (Regions 1, 3, 5) showed lower historic change rates than regions with marsh loss (2, 4) (Fig. 9, 1949-2015). This observation highlights a problem: with marsh removal, the back-barrier area will likely see an increased rate of erosion. In response to more erosion, an increase in shoreline modifications are anticipated as has been noted (Fig. 10).

A logical follow-up question is, how can shoreline erosion be mitigated? Based on historical photograph analysis, bulkhead creation in response to shoreline erosion is common in the Rodanthe back-barrier. Work by Currin and others (2010) noted no reduction in permitting for bulkheads in North Carolina. Yet research has shown that bulkheads, in fact, are often related to increased erosion and more loss of marsh (Douglass and Pickel, 1999; National Research Council, 2007). This results because bulkheads increase wave reflection and eventually scour which has been shown to reduce the width of the nearshore environment and cause the destruction of nearshore tidal zones (Douglass and Pickel, 1999; Riggs, 2001; National Research Council, 2007). Bulkheads also are known to inhibit landward migration of marsh vegetation, thereby leading to net marsh loss (National Research Council, 2007). For this reason, although the use of bulkheads in the study area may minimize short-term erosion, the long-term sedimentological (increased nearshore erosion) and ecological impacts (loss of marsh) suggest the need for a more sustainable alternative.

The living shoreline approach to shoreline stabilization employs artificial methods (e.g. sills, vegetation planting) to increase stability of natural shoreline habitats and may mitigate marsh loss in the study area (Fig. 17) (Currin et al., 2010; Bilkovic and Mitchell, 2013). Living shoreline methods can sustain and rehabilitate present shorelines; this provides an alternative to common hardening methods (e.g. bulkheads) (Currin et al., 2010). Maintaining marsh shoreline instead of bulkheads also sustains necessary estuarine nutrient cycling such as denitrification (O/Meara et al., 2015). Back-barrier shorelines in Rodanthe would benefit from marsh sills that mitigate modern marsh loss and vegetation planting which encourages new marsh growth. Each of these shoreline stabilization methods are recommended by the NC Department of

Environmental Quality for shorelines with moderate to large fetch in the Pamlico Sound (NCDEQ, 2013).

Additional options could be construction of oyster or oyster cultch reefs, as these offer natural alternatives to rock sills (Currin et al., 2010). Oyster reefs were historically present in Pamlico Sound and constructed intertidal reefs with native eastern oyster have proven successful restoration efforts (Powers et al., 2009). Reefs also operate as breakwaters and may have the same effect as sills when mitigating storm impacts on shoreline (Scyphers et al., 2011; Gittman et al., 2014). Work by Meyer and others (1997) on marshes with adjacent oyster cultch suggests positive impacts. There was significantly higher accretion in cultch-protected marsh than unprotected marsh. The use of oyster reefs would provide a natural method of reducing wave impact on the Rodanthe shoreline while restoring significant oyster habitats.

5.1.1 Sediment Fluxes and Storage

Utilizing the scarp and shoreline data, the three methods estimated a significant volume of sediment generated by erosion and likely supplied to the study area (760 to 1,900 $m^3\ y^{-1}$) However, it is worth noting that the annual volume estimates were substantially less than the calculated sedimentation in the emergency ferry channel for Hurricane Irene (14,000 m^3). This highlights the magnitude of storm remobilized sediments. The predominance of deposition within sectors 1 and 2 (near shore sectors) of the ferry channel, suggests remobilized storm sediments are locally transported and deposited. With such a high volume of sediments resuspended during large wind events (e.g., hurricanes), fine-grained sediments eroded from the shoreline may be transported beyond the study area.

Moreover, the VCR from method 3 (-970 m^3 y^{-1}) when distributed across the study area (32 km^2) yielded a layer of only <30 μm y^{-1} (~97,000 m^3 total shoreline erosion over 66 years). Based on this calculation, sediment eroding from the shoreline may not be sufficient to cause much, if any, accretion. With a low annual shoreline sediment supply to the region, sediment deposition in the ferry channel may be due from local sediment remobilization during storms (e.g., Irene). The deposition from Irene (14,000 m^3) taken from the study area would amount to 400 μm of vertical sediment loss. Thus, dredging of the channel following storms and emplacement of this material on land may represent an important net loss of sediment in the back-barrier study area. Perhaps, a Regional Sediment Management (http://rsm.usace.army.mil/) perspective should be taken and some or all of this material should remain (i.e., be replaced) in the back-barrier system.

5.2 Sediment Character and Remobilization

Previous research identified the Hatteras Flats region of the Outer Banks as a sandy, subtidal flat of reworked and coalesced flood tidal deltas (Culver et al., 2006; Mallinson et al., 2010; Mallinson et al., 2011; Riggs et al., 2011; Peek et al., 2013). Data from this study support this idea. With only one sample with >5% mud (found at the deepest depth sampled, 4.1 m), this shallow subtidal area is dominated by fine to medium sandy surface sediments (Fig. 11). Nevertheless, grain size varies spatially in the study area. Finer samples are generally found in deeper waters, especially in the north and northwest sector of the grid. Larger grain sizes were seen closer to shore due to shoaling and an increased impact of waves as they transition to shallow water (Mason, 2010). Change in the grain sizes between the first collection (June) and

the second (December) showed very little change (< 0.4 phi change between samples) suggesting little short-term (sub-annual) change.

Both marsh and SAV habitats across the back-barrier are capable of producing organic matter and can induce organic-rich sediments (Mcleod et al., 2011; Fourqurean and Serrano, 2012). However, with extremely low loss on ignition values (<1%), it appears the study area does not store high organic sediment (D'Andrea et al., 2002; Swerida, 2013). Eroding marshes undoubtedly provide a source of organic matter to estuarine sediments (Canuel and Hardison, 2016). A few samples that were taken directly from marsh scarps showed high LOI (6-25%). The lack of LOI in the back-shore sediments compared to the marsh samples suggests eroded organic material must be dispersed beyond the area, consumed or moved onto the barrier.

Sediment transport in the APES has been reported to be dominated by wind-driven resuspension and weak wind-driving circulation due to the low tidal range (generally <30 cm in the system) (Wells and Kim, 1989; Benninger and Wells, 1993; Dillard, 2008). Observations indicate that sediments in the back-barrier are likely remobilized during strong wind events by both waves and currents, with large sediment transport occurring during storm events (e.g., Fig. 11, 12), especially hurricanes like Isabel, Ophelia and Irene. Wave and current data from the August-September 2015 deployment showed bed shear stresses exceeding the critical shear stress for motion of fine sands (Fig. 13). Note, each exceedance event occurred during sustained winds along a SW-NE trend (i.e., SW for wave event; NE for current event), which is the greatest fetch extent for wave generation in the Pamlico Sound. Sediment transport in these events will follow the currents and indicate transport onshore during SW winds and offshore during NE winds (Fig. 13). With strong SW winds following storm events, sediments may be transported onshore after storm departure (Fig. 12). Although the period of instrument

deployment did not include a major storm, it suggests some episodic sediment resuspension and redistribution during non-storm weather conditions as well.

Bathymetric surveys of the emergency ferry channel suggest the importance of major storms. Several survey periods show large bathymetry change. These shoaling changes occur across survey periods with hurricanes (i.e. Isabel, Ophelia, Irene). The high energy wind (>20 m s^{-1}) and wave processes in these hurricanes were likely ideal for sediment redistribution in the back-barrier (Fig. 12).

5.3 SAV Habitat Properties

The persistent depth zone of SAV in this study (0.5-2.2 m) is somewhat different than reported elsewhere (Short et al., 2002; Orth et al., 2010; Angradi et al., 2013). Depth ranges for SAV vary greatly across the eastern U.S. as a result of varying water quality conditions (Short et al., 2002). Previous studies suggest SAV habitats are largely controlled by depth due to light dependence (Hall et al., 1999; Koch et al., 2001; Short et al., 2002; Angradi et al., 2013; Findlay et al., 2014). Other studies found that SAV habitats were generally shallower than 1 m below mean low water level (Angradi et al., 2013; Findlay et al., 2014). An SAV habitat depth range of 0.3 – 1.3 m would be expected in the study area if water level was controlled by tide alone. Water level data from the instrument deployment in Rodanthe shows a region affected by tides and influenced by wind (Fig. 13). Wind-influenced water level changes may prevent shallower habitat growth (>-0.5) in study area shoals by increased subaerial exposure during strong NE wind events (Short et al., 2002; Palinkas and Koch, 2012; Angradi et al., 2013), and the deeper depth is likely because of the relatively clearly water in the area.

Low organic content in the sediment samples contradicts past research; higher carbon sequestration is common in SAV beds. With 30-45% of the study area covered by SAV, both allochthonous and autochthonous organic carbon is expected to be present (Kennedy et al., 2010; Mcleod et al., 2011; Fourqurean and Serrano, 2012). Other studies hypothesize persistent SAV habitats are characterized by low organic matter (Fig. 6) (Wicks et al., 2009; Palinkas and Koch, 2012). The near-zero organic matter content in the study area suggests there is not high carbon storage in the sediments surrounding SAV. The low (<1.5%) LOI in all sediment samples within Rodanthe SAV habitat is attributable to either low productivity or frequent sediment flushing and may contribute to SAV extent stability. This study did not address in situ organic matter production or destruction, but wave and current data suggest remobilization events are episodic and may remove organic matter from SAV habitat.

6.0 CONCLUSION

Through analysis and comparison of shoreline dynamics, sediment properties, bathymetry, and submerged aquatic vegetation mapping this study yielded three conclusions regarding the Rodanthe back-barrier:

(1) Shoreline erosion was the dominant shoreline change process across the study area and areas of high erosion rates showed increased anthropogenic modification. As marsh shorelines erode and are replaced with sediment banks, shoreline erosion is expected to continue and possibly increase until bulkheads and rip-rap exceed natural shoreline presence or shoreline hardening occurs. Living shoreline methods (nourishment, sills and vegetation planting) may prove a better alternative to bulkheads for reducing back-barrier erosion. Sediment flux from the shoreline would have produced less than 30 $\mu m\ y^{-1}$ of accretion across the basin, which does not appear to be a significant sediment source in the offshore back-barrier.

(2) Resuspension events remobilize sediments by current or wave processes, and these events likely maintain largely mud-free sands along the back-barrier by removing supplied muds and organic matter. Shear stress exceeded τ_{cr} during stronger winds of the instrument deployments, suggesting that waves and currents episodically resuspend sediments during moderate wind conditions (>10 $m\ s^{-1}$). Times of moderate waves indicate that forces associated with currents exceed τ_{cr}. Paired with the low LOI and mud percent, resuspension events provide a mechanism for the local transport of sands. Channel bathymetry data suggest large local sediment deposition events occur associated with storms, requiring dredging operations to maintain navigable waters for ferry access to the island. In the future, the option of placing dredged sediment in the system should be considered, potentially as nourishment for eroding shorelines.

(3) The optimal depth of SAV habitats at Rodanthe is 0.5-2.2 m due to wind-influenced water levels and light limitation. Persistent SAV habitat was mapped throughout the back-barrier shoal system where low mud percentages and organic matter are observed. Wind tides affect water level along with astronomical tides and likely influence SAV distribution due to subaerial exposure of nearshore shallow habitat. The large area of SAV recurrence across a decadal period suggests habitat stability with regards to wave and current resuspension, as well as sediment properties (e.g., low mud, low organic matter). The lack of organic matter in an area of persistent SAV may indicate low carbon storage potential for the Rodanthe SAV habitat.

The study area represents an active back-barrier environment characterized by shoreline erosion and episodic remobilization of sediments. Understanding sediment dynamics is necessary to maintain a healthy back-barrier from shoreline to SAV habitat.

Table 1: Shoreline Change Rates

Year	Mean Change (m)	Mean Change Rate (m y^{-1})
1949-1974	-9.3 ± 3.5	-0.38 ± 0.14
1974-2007	-15.4 ± 1.6	-0.47 ± 0.14
2007-2012	-0.6 ± 1.6	-0.10 ± 0.32
2012-2015	-3.5 ± 1.7	-0.98 ± 0.56
1949-2015	-27.9 ± 2.1	-0.41 ± 0.03

Table 2: Change of Loss on Ignition (%) of Resampled Sites in 2015.

Station ID	June	Dec	% ΔLOI
1	0.24	0.56	133
7	0.28	0.53	89
13	0.17	0.46	171
33	0.19	0.46	142
39	0.33	0.62	88
41	0.20	0.37	85
43	0.24	0.56	133
45	0.58	0.79	36
55	0.21	0.34	62
59	0.16	0.33	106
61	0.20	0.37	85
63	0.41	0.75	83
75	0.19	0.35	84
79	0.22	0.59	168

Table 3: SAV Coverage Area

Year	Coverage (km^2)
2004	30.8
2005	24.8
2009	28.7
2010	29.8
2014	29.5

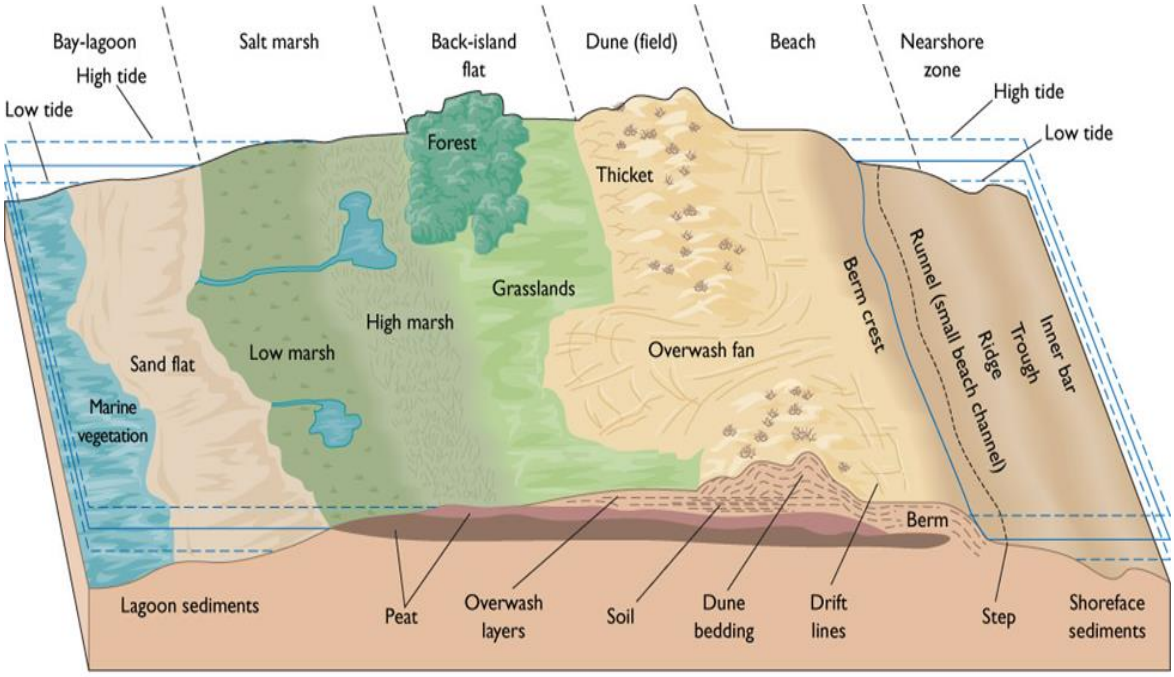

Figure 1: A cross section of an idealized barrier island. The focus of this project is the back-barrier region extends from the lagoon (or bay or sound) to the back-island flat. (http://www.geo.arizona.edu/geo4xx/geos412/OcSci07.Coastal.pdf)

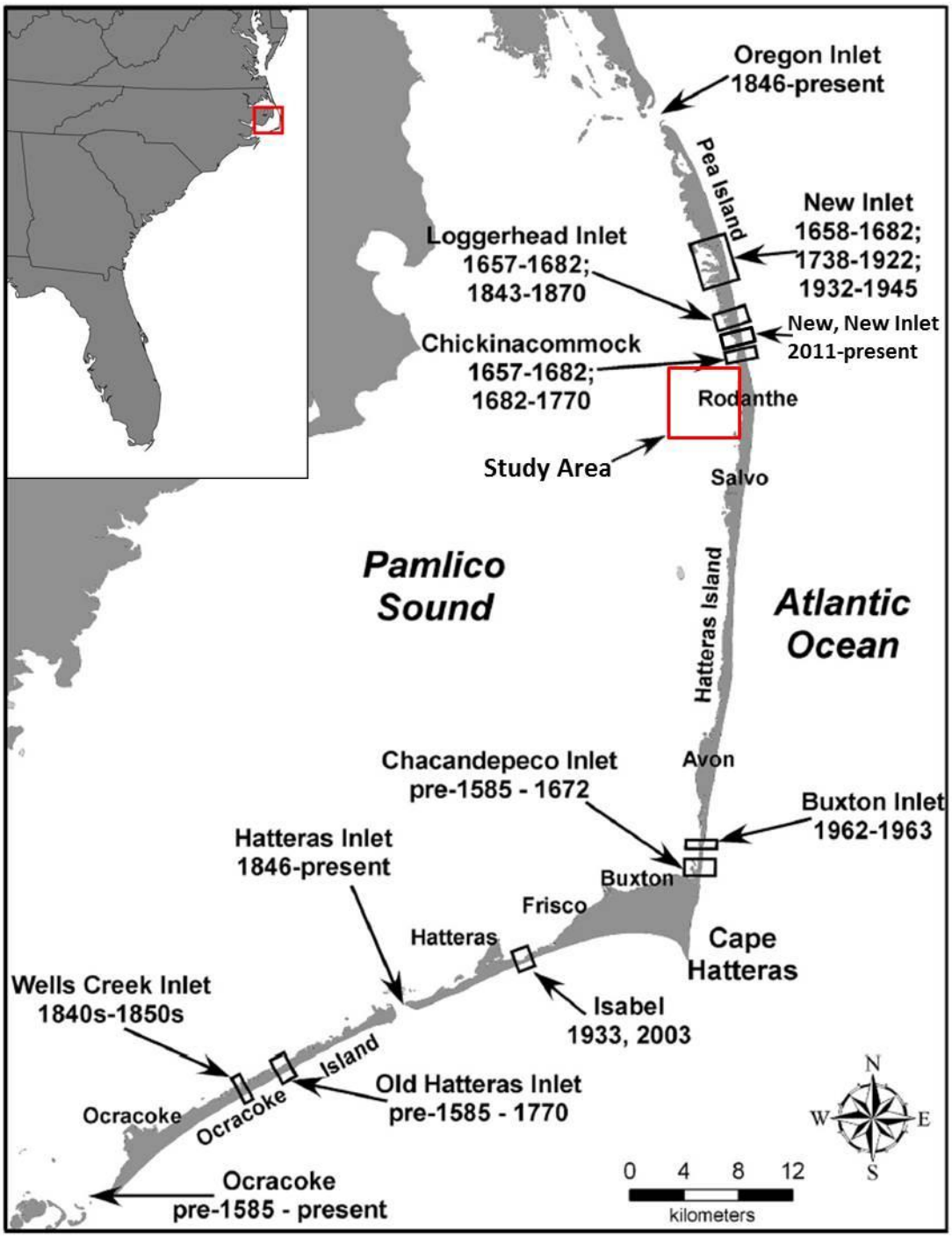

Figure 2: Historic and present inlets in the Outer Banks. Modified from Mallinson et al., 2010. Note the location of the study area.

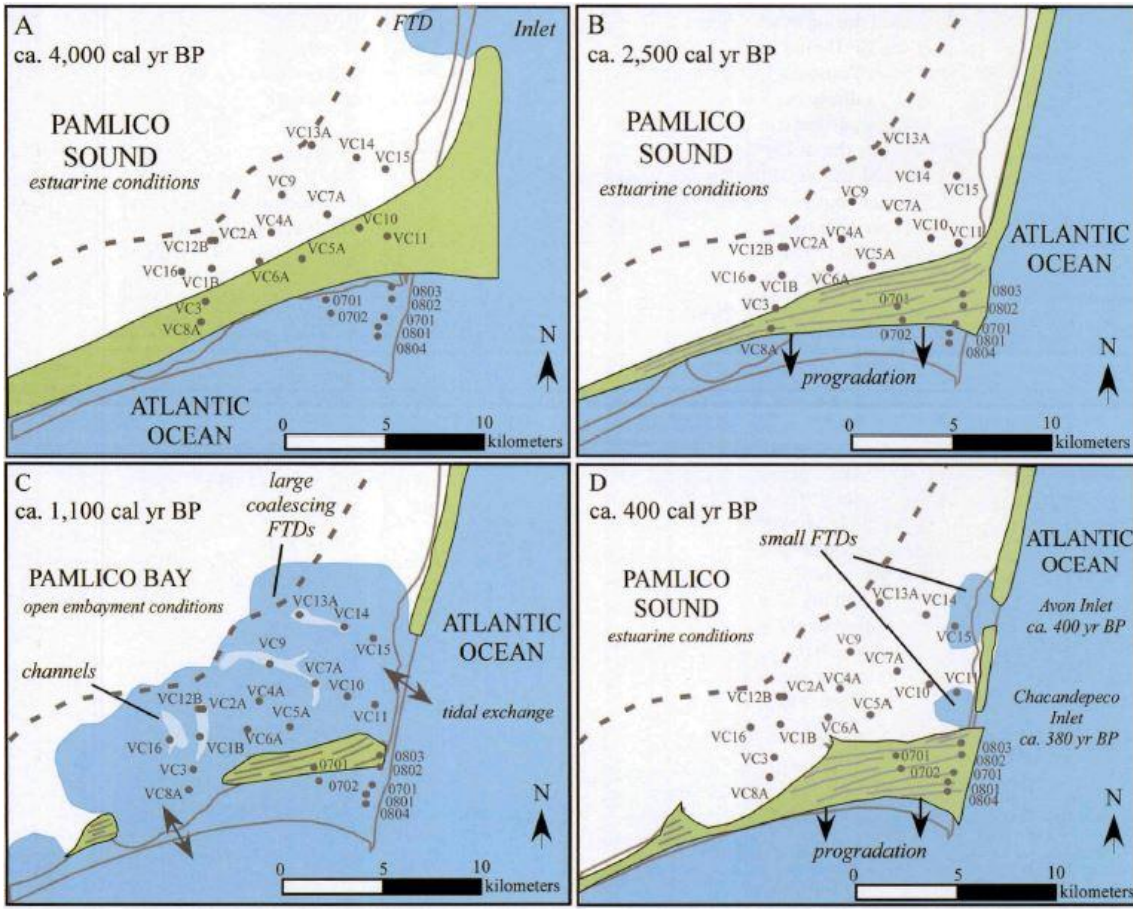

Figure 3: Holocene evolution of the southern Hatteras Flats during open marine exchange between Pamlico Sound and the Atlantic Ocean (Peek et al., 2013). This shows the development of the coalesced flood tidal deltas (FTD) that create bathymetric topography on the flats south of the study area.

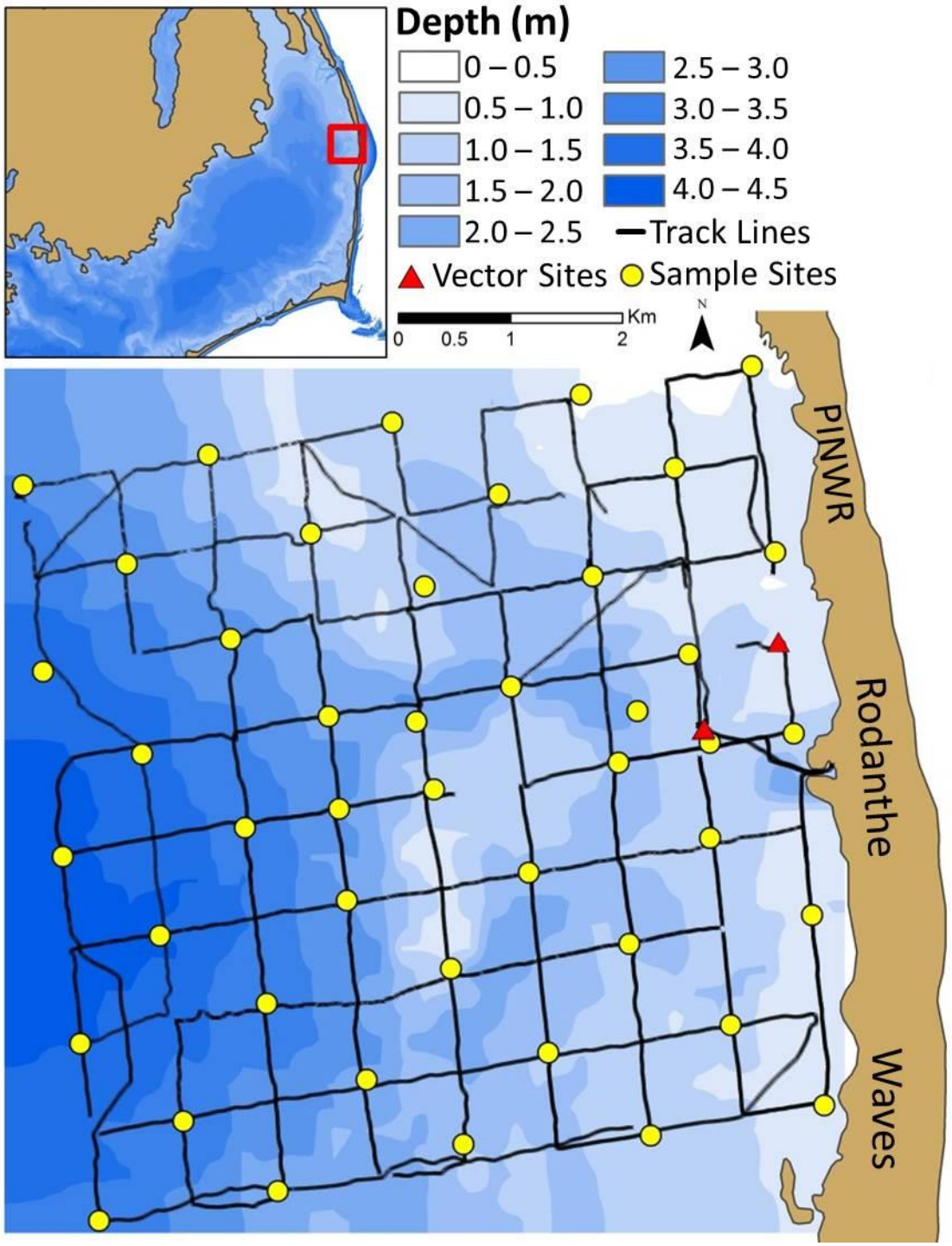

Figure 4: The back-barrier study area near Rodanthe, NC. Bathymetry was mapped using a single-beam echosounder (track lines shown as solid black line). Sites where currents and waves were measured with a Nortek Vector are noted by red triangles. Sediment sample sites are shown with yellow circles.

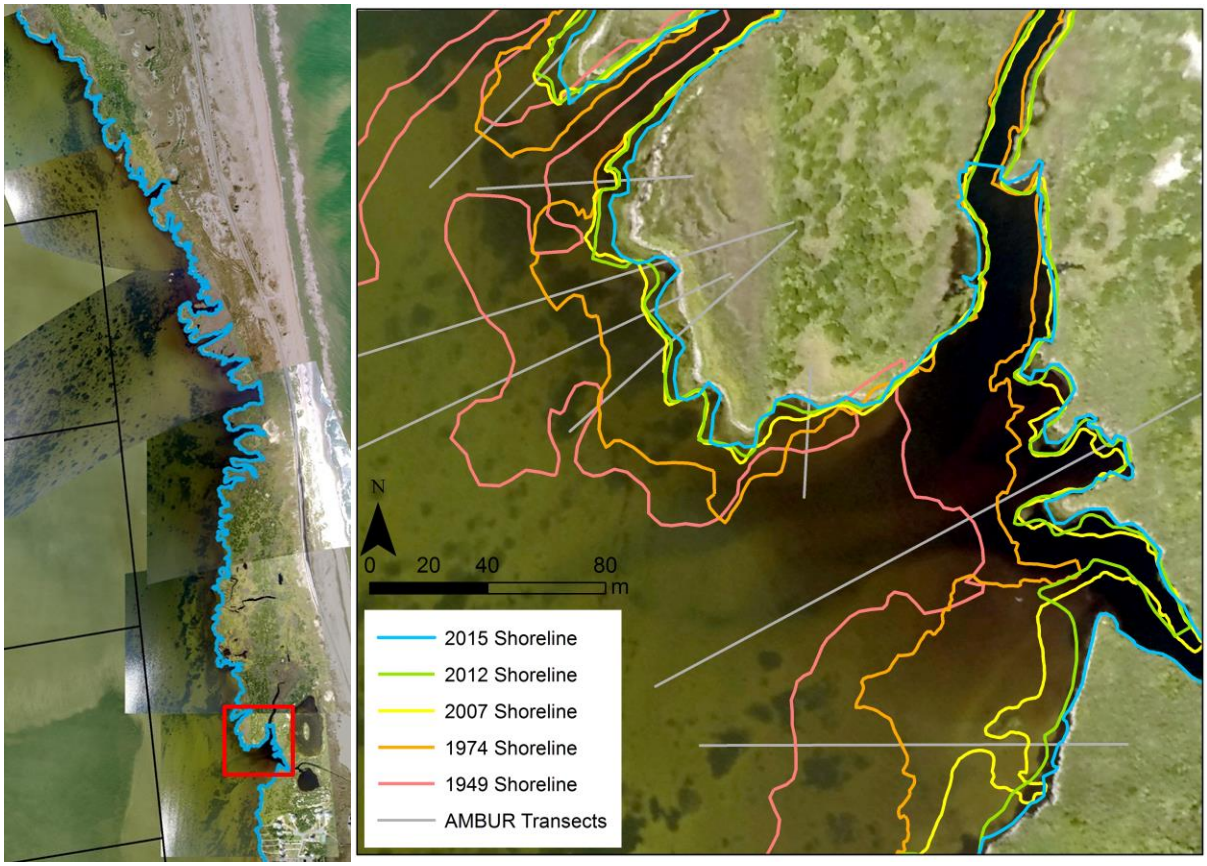

Figure 5: Mapping of the 2015 shoreline with aerial photography (left) and example of shoreline change over time for area highlighted in the red box (right).

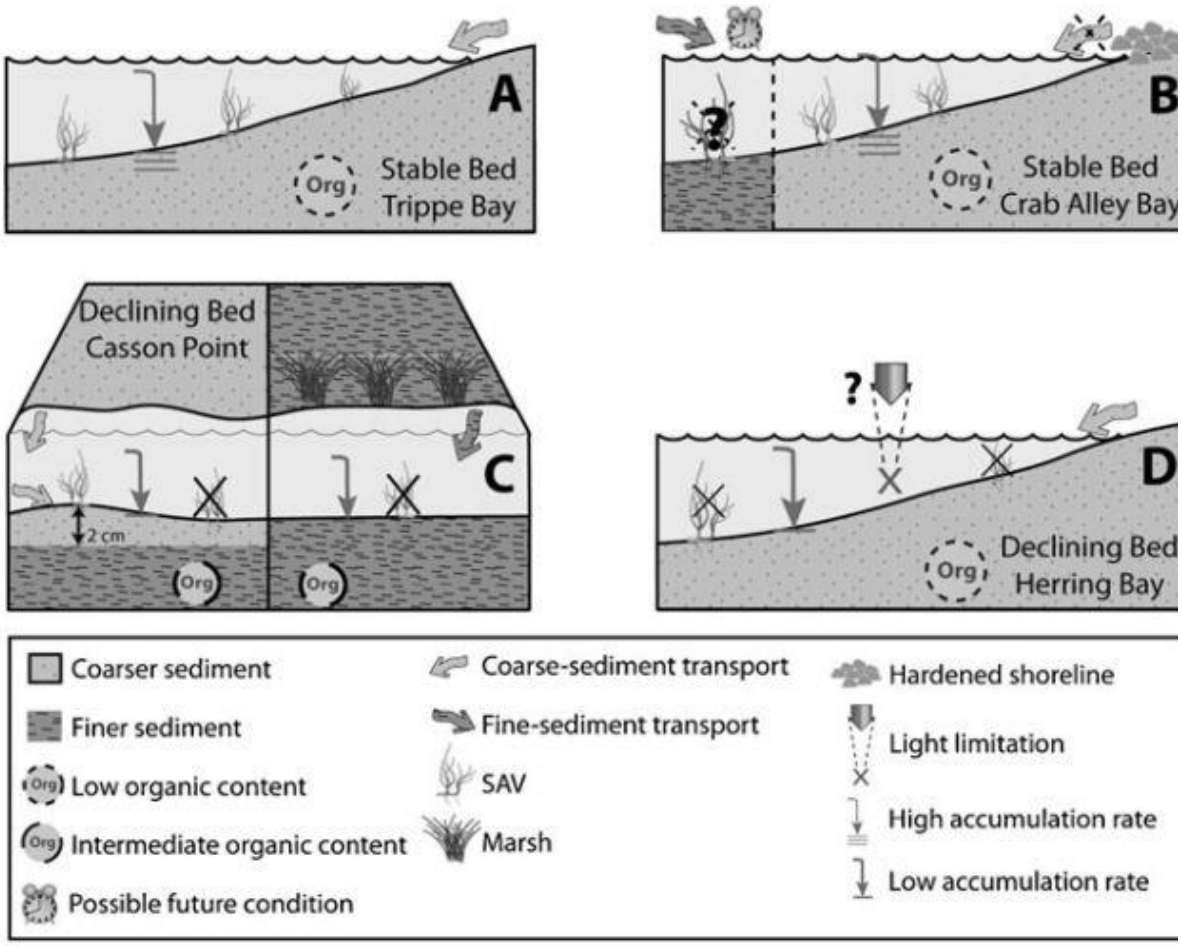

Figure 6: Conceptual models for persistent (top) and ephemeral (bottom) SAV beds (Palinkas and Koch, 2012). These models suggest the importance of sand presence in SAV beds to facilitate frequent water exchange around SAV roots. They also show removal of SAV when organic content is too great and enables SAV uprooting during high wave and current conditions.

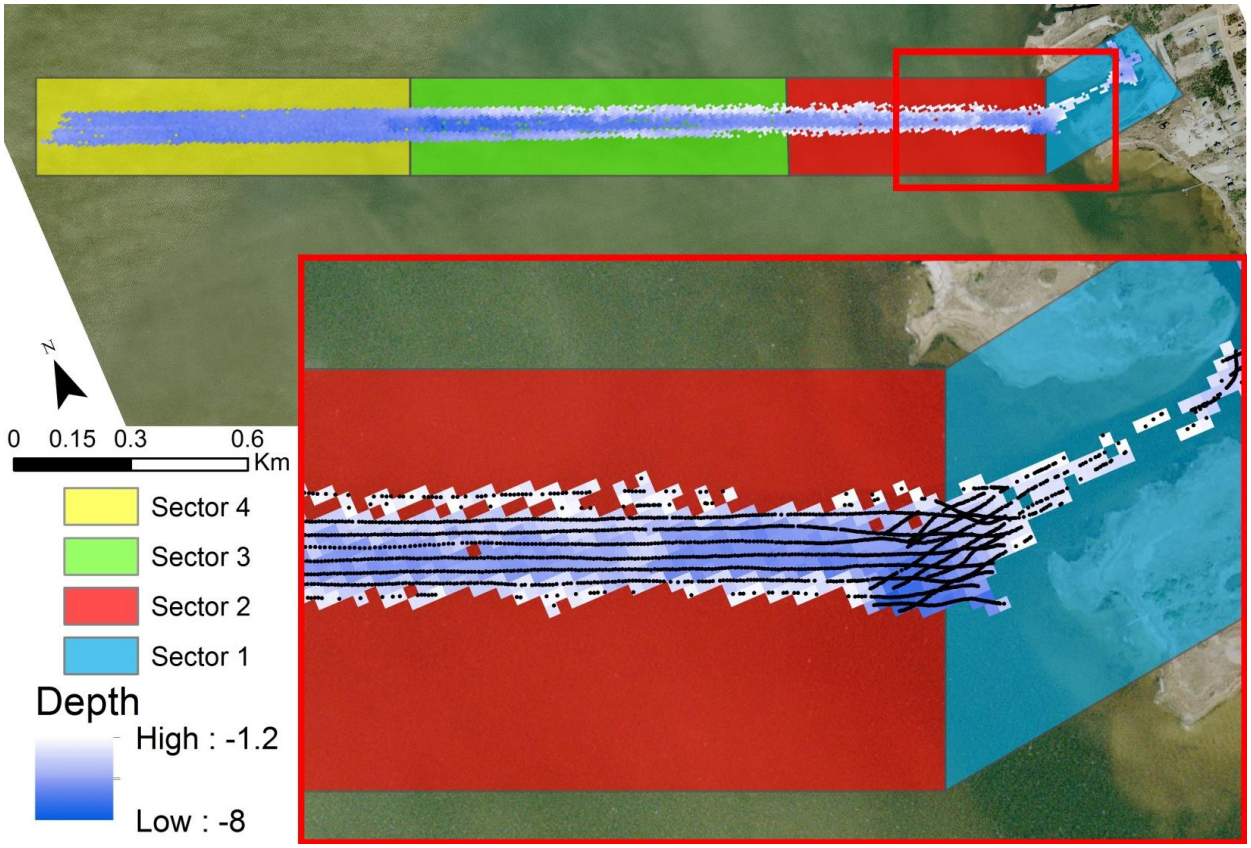

Figure 7: Example measured bathymetry for 2000 in the emergency ferry channel approaching Rodanthe. Data shown is derived from a Kriged bathymetry survey (black point data). Sectors were defined to evaluate spatial change in the channel. These maps were created for several years between 1995 and 2014.

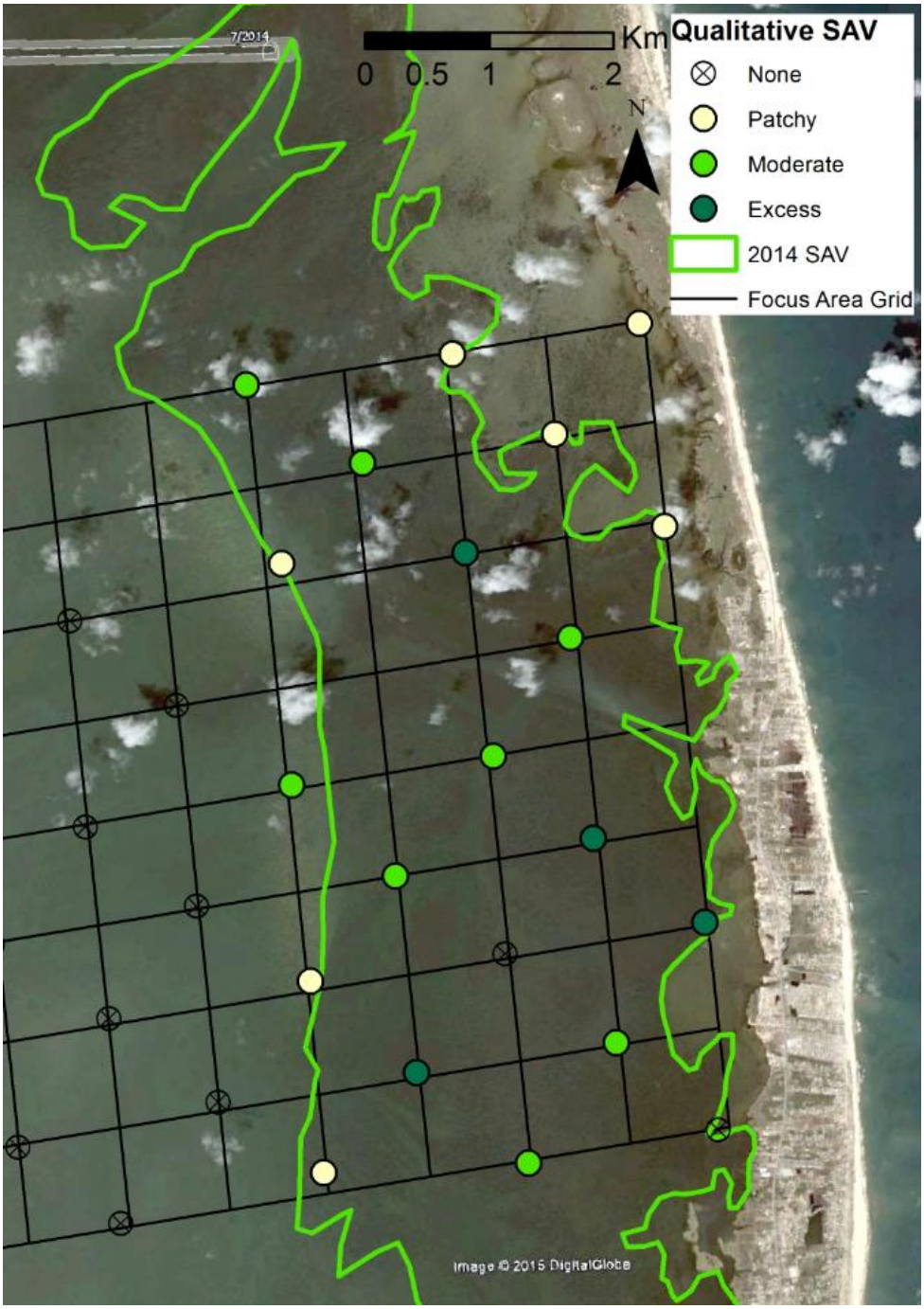

Figure 8: Example of SAV area mapped by heads-up digitization and 2014 qualitative SAV survey. Note the dark shades indicating the SAV in shallow water. The qualitative survey agreed with SAV boundary digitization.

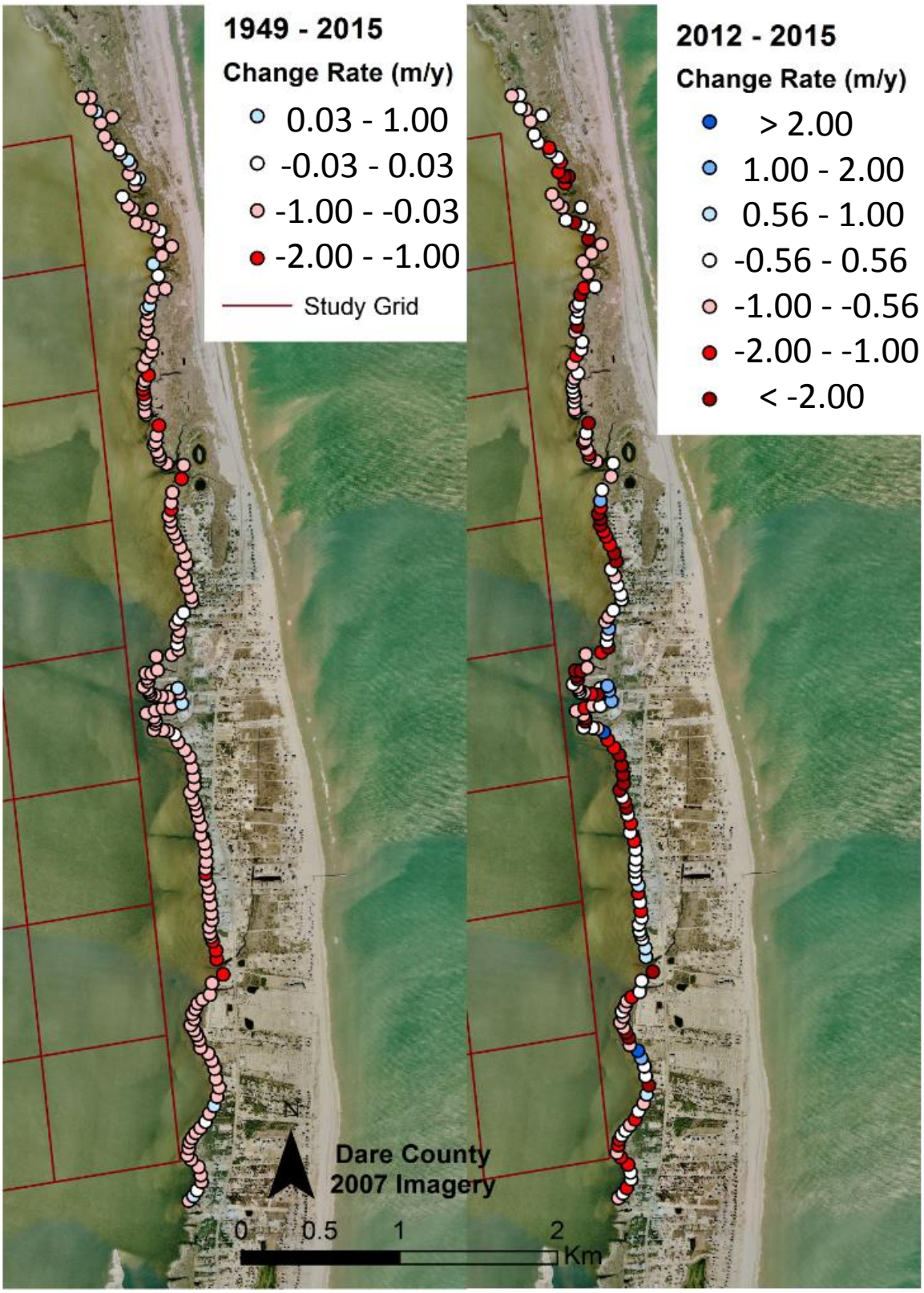

Figure 9: Shoreline change rates for 1949-2015 (left) and 2012-2015 (right). Note the widespread erosion.

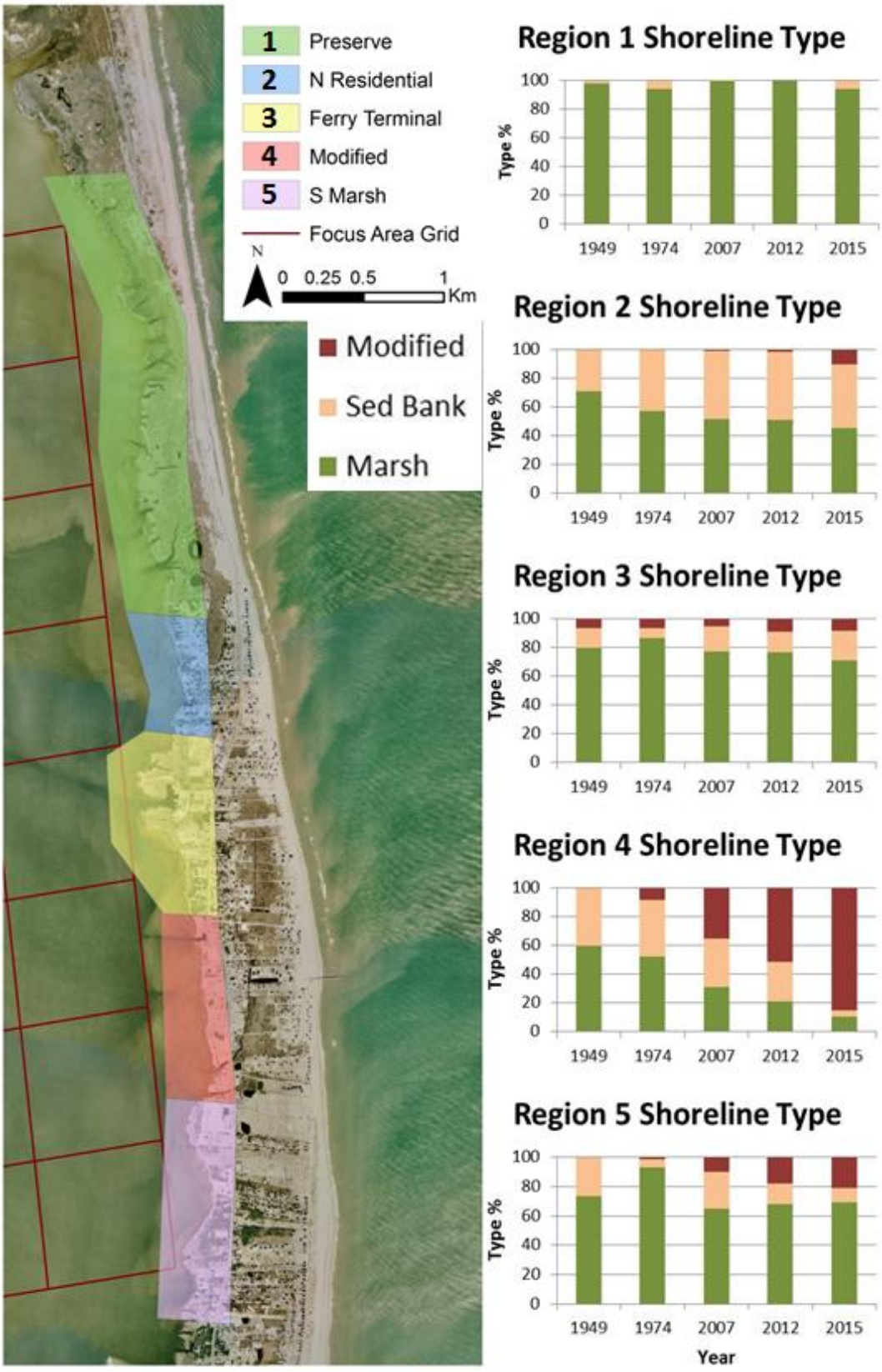

Figure 10: Shoreline type change for each region for all time steps.

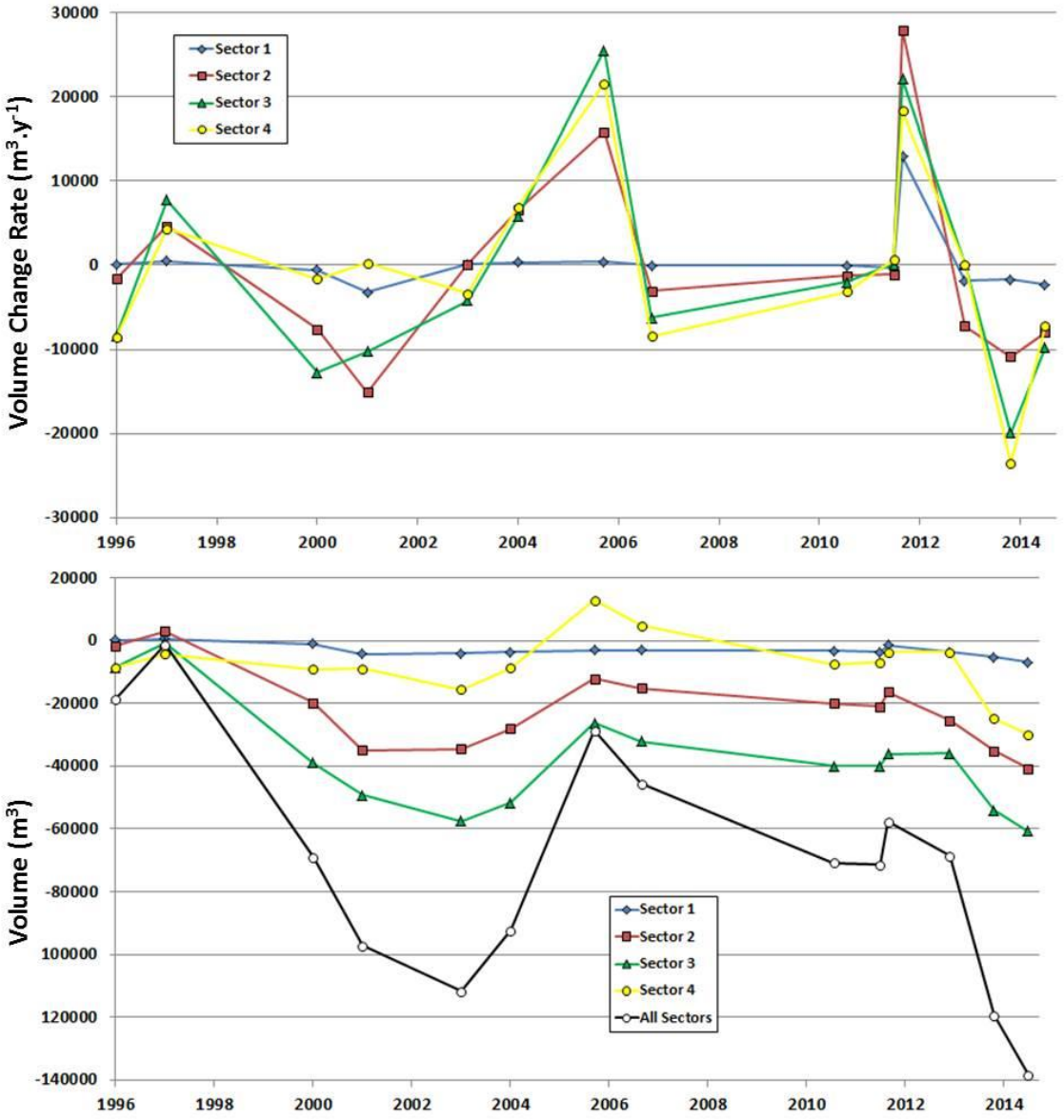

Figure 11: Channel volume change between time steps (top, m^3/y), adjusted for the length of time between each step. Cumulative volume change (bottom) for the channel by sector and for all sectors combined. Note the large increases in 2003-2005 and 2011.

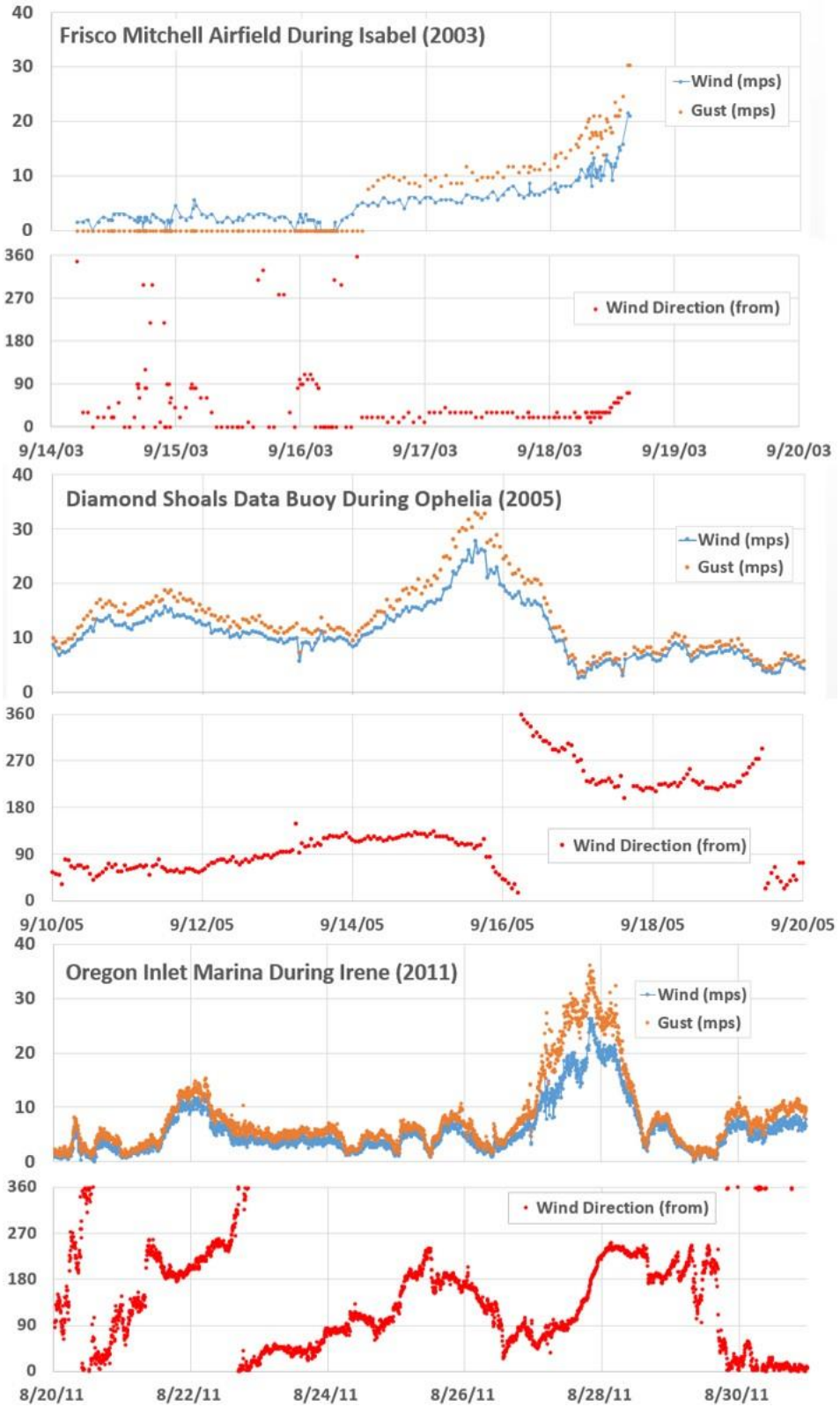

Figure 12: Meteorological data for Ophelia (top), Isabel (middle), and Irene (bottom). Each show winds and gusts exceed 20 m/s (or m s^{-1}) within storm onset and SW winds following storm departure. Data sources are varied due to station outages during storms.

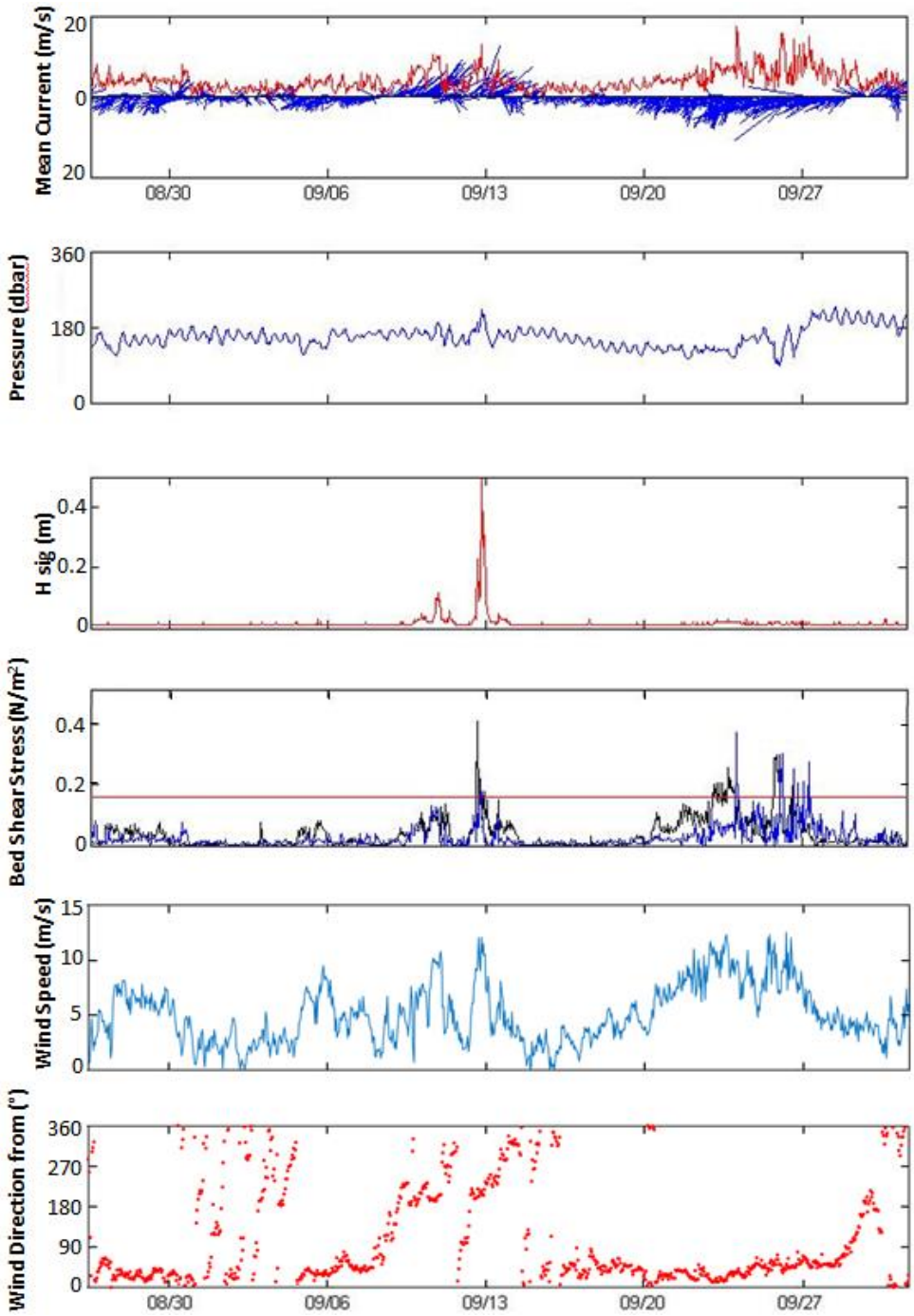

Figure 13: Measured hydrodynamic data from the vector deployment. Mean currents are shown as magnitude (red) and direction (blue). Pressure shows changes in water level. Bed shear stresses exceeded τ_{crit} (0.18 N/m^2, red line) for two wind events. The first event showed high H_s where the latter event showed very low H_s and high currents. Each period of high shear stress was during winds >10 m s^{-1}. Sediment transport direction is onshore in the first event (SW wind) and offshore in the second event (NE wind).

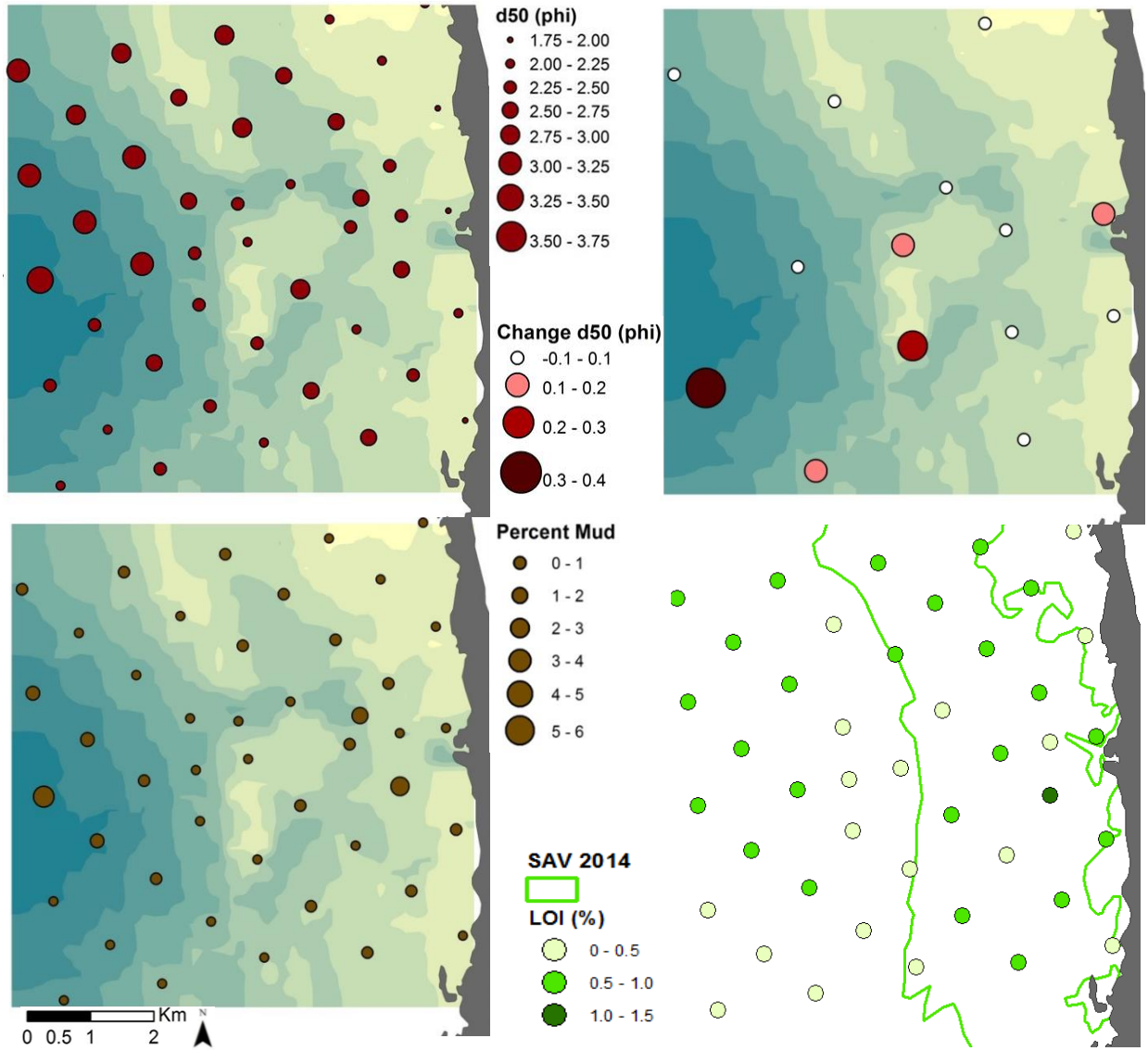

Figure 14: d50 of sediment samples (top left). Change of d50 (top right). Percent mud in samples (bottom left). Loss on ignition as a proxy for organic content (bottom right). Sediments were fine to medium sands with low mud and organic content. Samples showed little change between sampling periods.

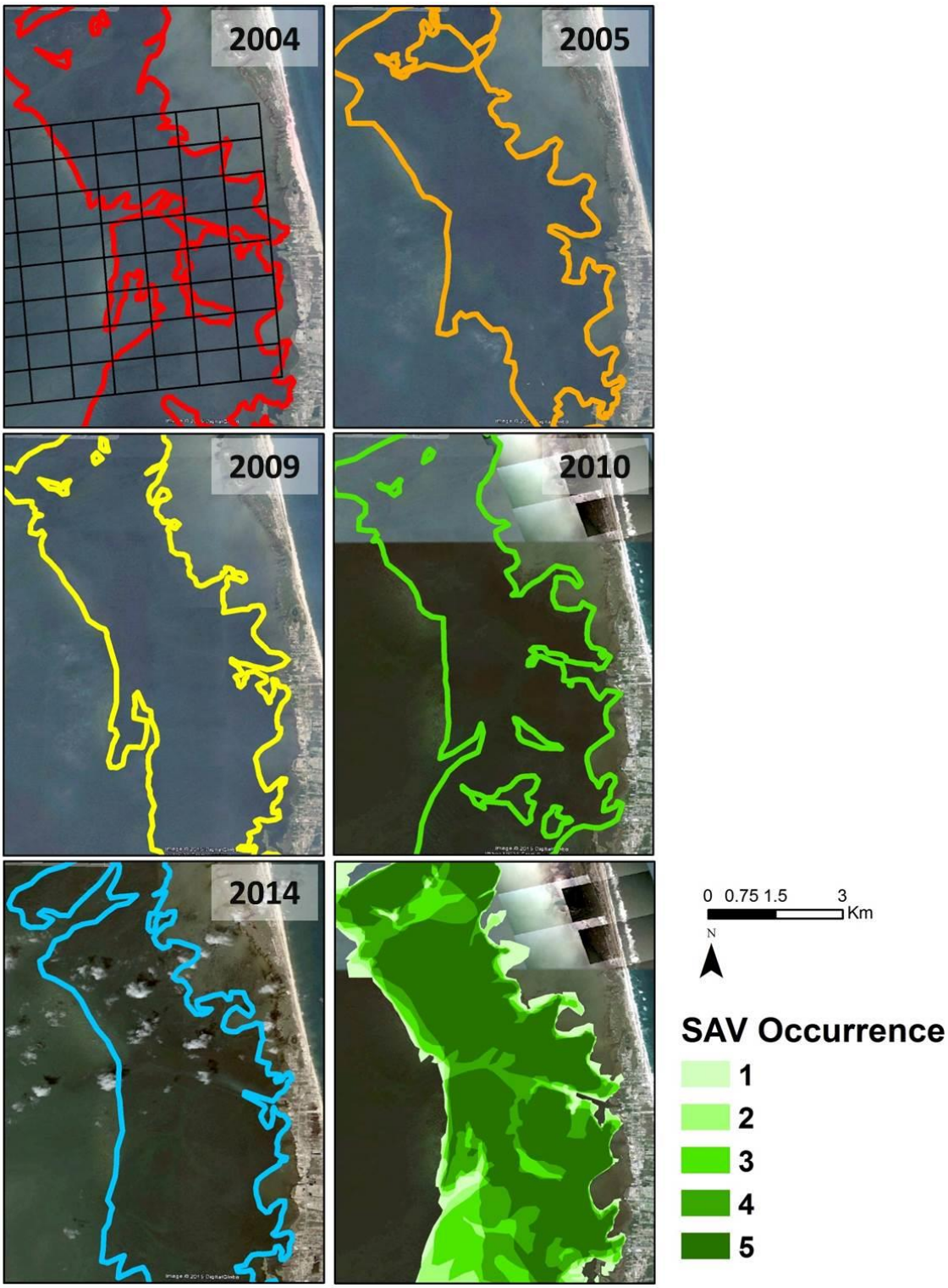

Figure 15: Heads-up mapped SAV boundaries for all time steps. Study area grid is shown in the 2004 data. (Bottom right) Occurrence of SAV between all time steps. Occurrence = 1 means SAV was only present during 1 year mapped. Occurrence = 5 means SAV was present at all years mapped. Data show persistent coverage of SAV with moderate variability between years.

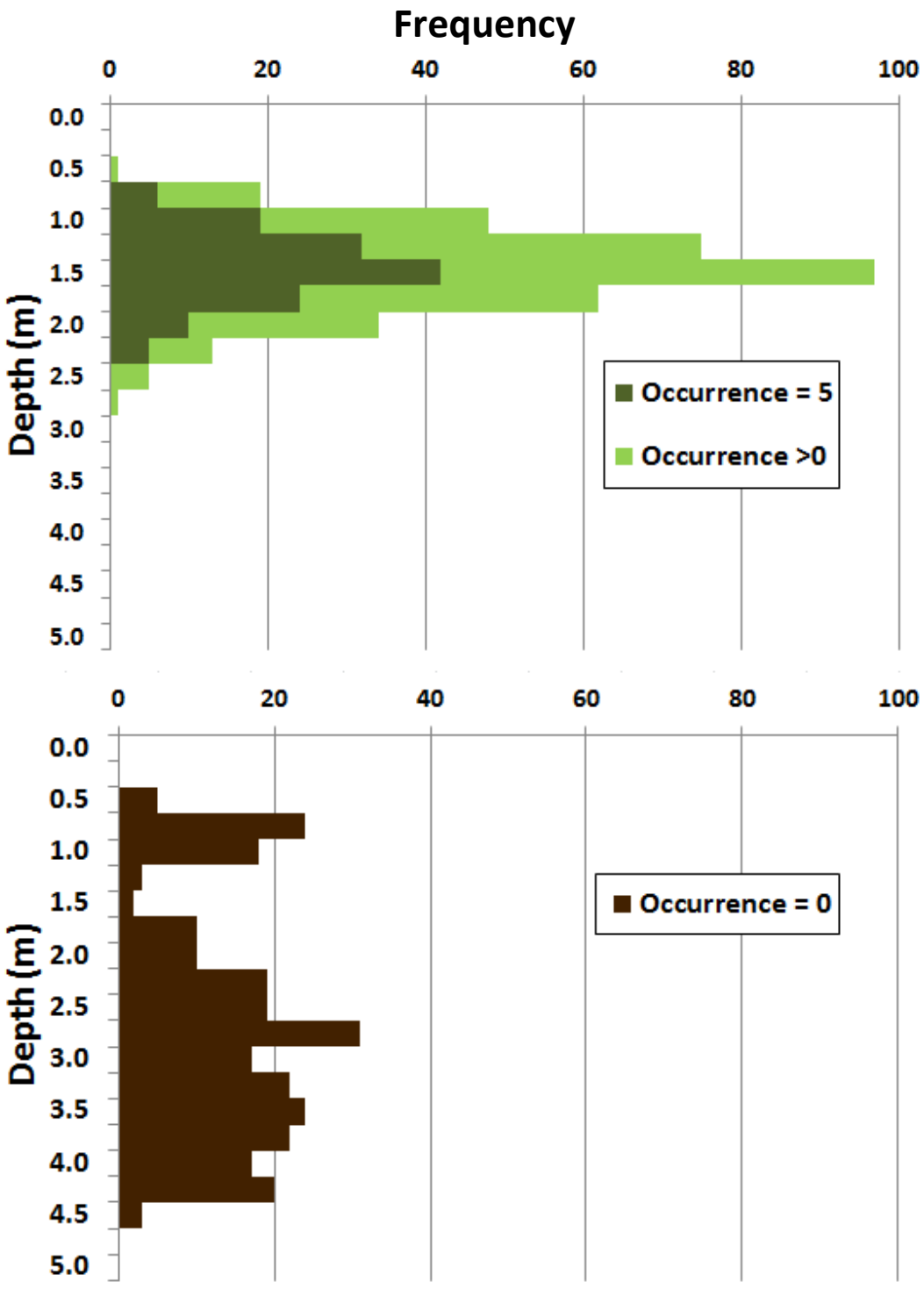

Figure 16: SAV frequency with depth (top) and depth values without SAV (bottom). Occurrence of 5 shows SAV persistent across all maps. Occurrence > 0 shows SAV presence during at least one map. The depth range of persistent SAV was 0.5-2.2 m, and all SAV was 0.4-2.7 m.

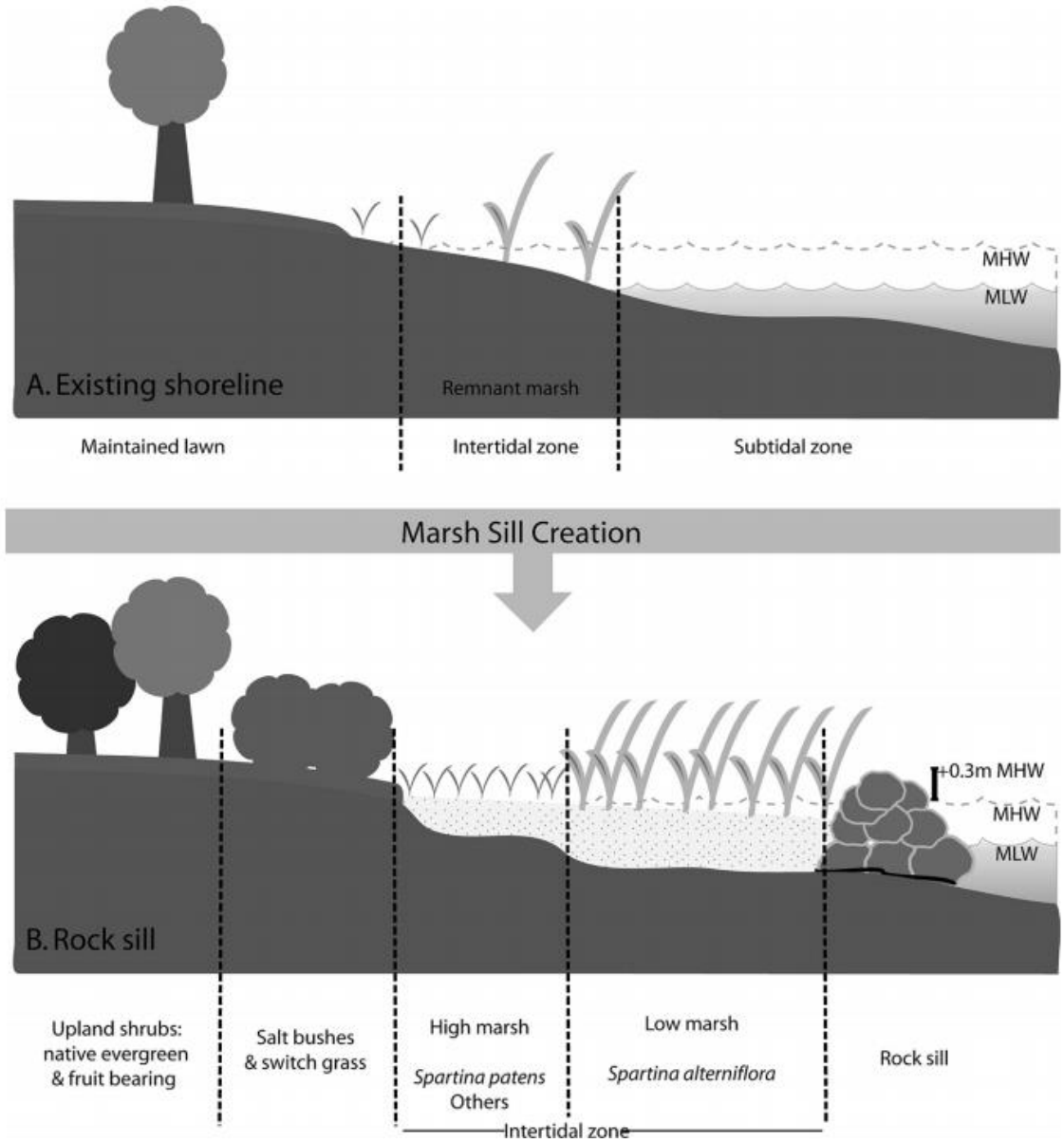

Figure 17: Example marsh-sill living shoreline stabilization method (Bilkovic and Mitchell, 2013). This method places a sill to protect current marsh and promote natural vegetation stabilization.

Literature Cited:

Adair, S. E., Moore, J. L., & Onuf, C. P., 1994. Distribution and status of submerged vegetation in estuaries of the upper Texas coast. Wetlands, 14(2):110-121.

Angradi, T. R., Pearson, M. S., Bolgrien, D. W., Bellinger, B. J., Starry, M. A., Reschke, C., 2013. Predicting submerged aquatic vegetation cover and occurrence in a Lake Superior estuary. Journal of Great Lakes Research 39:536-546.

Austin, M. J., Masselink, G., 2008. The effect of bedform dynamics on computing suspended sediment fluxes using optical backscatter sensors and current meters. Coastal Engineering 55:251-260.

Bartholdy, J., Aagaard, T., 2001. Storm surge effects on a back-barrier tidal flat of the Danish Wadden Sea. Geo-Marine Letters 20:133–141. doi:10.1007/s003670000048

Bell, S. S., Robbins, B. D., Jensen, S. L., 1999. Gap Dynamics in a Seagrass Landscape. Ecosystems 2:493-504.

Benninger, L. K., Wells, J. T., 1993. Sources of sediment to the Neuse River estuary, North Carolina. Marine Chemistry 43:137-156.

Bilkovic, D. M., Mitchell, M. M., 2013. Ecological tradeoffs of stabilized salt marshes as a shoreline protection strategy: Effects of artificial structures on macrobenthic assemblages. Ecological Engineering 61:469-481.

Biribo, N., Woodroffe, C. D., 2013. Historical area and shoreline change of reef islands around Tarawa Atoll, Kiribati. Sustainability Science 8:345-362.

Blott, S. J., Pye, K., 2001. GRADISTAT: A grain size distribution and statistics package for the analysis of unconsolidated sediments. Earth Surface Processes and Landforms 26:1237-1248.

Blunt, J. A.C., Larcombe, P., Jago, C. F., 1999. Quantifying the response of optical backscatter devices and transmissometers to variations in suspended particulate matter. Continental Shelf Research 19:1199-1220.

Booth, J.G., Miller, R.L., McKee, B.A., Leathers, R.A., 2000. Wind-induced bottom sediment resuspension in a microtidal coastal environment.pdf. Continental Shelf Research 20:785–806.

Canuel, E. A., Hardison, A. K., 2016. Sources, ages, and alteration of organic matter in estuaries. The Annual Review of Marine Science. Doi: 10.1146/annurev-marine-122414-034058.

Chanson, H., Reungoat, D., Simon, B., Lubin, P., 2011. High-frequency turbulence and suspended sediment concentration measurements in the Garonne River Tidal Bore. Estuarine Coastal and Shelf Science 95:298-306.

Chen, S.-N., Sanford, L.P., Koch, E.W., Shi, F., North, E.W., 2007. A nearshore model to investigate the effects of seagrass bed geometry on wave attenuation and suspended sediment transport. Estuaries and Coasts 30:296–310.

Clinch, A. S., Russ, E. R., Oliver, R. C., Mitasova, H., Overton, M. F., 2012. Hurricane Irene and the Pea Island Breach: Pre-storm site characterization and storm surge estimation using geospatial technologies. Shore and Beach Vol. 80, No. 2.

Condition Survey Rodanthe Harbor, July 15, 2013. 1:3,600. Mapped by: DJM. Surveyed by: BRJ, DCH. U.S.Army Engineer District Corps of Engineers, Wilmington, NC.

Condition Survey Rodanthe Harbor, November 01, 2012. 1:3,600. Mapped by: MSA. Surveyed by: BRJ, DCH. U.S.Army Engineer District Corps of Engineers, Wilmington, NC.

Condition Survey Rodanthe Harbor, November 26, 2012. 1:3,600. Mapped by: DJM. Surveyed by: BRJ, DCH. U.S.Army Engineer District Corps of Engineers, Wilmington, NC.

Conery, I., 2014. Decadal-scale evolution of a barrier island: Insights from storm overwash and shoreline change on Ocracoke Island, NC. MS Thesis, East Carolina University.

Cowart, L., Walsh, J. P., Corbett, D. R., 2010. Analyzing estuarine shoreline change: a case study of Cedar Island, North Carolina. Journal of Coastal Research, 26:817-830.

Cowart, L., D.R. Corbett, J.P. Walsh, 2011. Shoreline Change along Sheltered Coastlines: Insights from the Neuse River Estuary, NC. Remote Sensing, 3, 1516-1534.

Culver, S.J., Ames, D., Corbett, D.R., Mallinson, D.J., Riggs, S.R., Christopher, S., Vance, D., 2006. Foraminiferal and Sedimentary Record of Late Holocene Barrier Island Evolution, Pea Island, North Carolina: The Role of Storm Overwash, Inlet Processes, and Anthropogenic Modification. Journal of Coastal Research 22, 836-846.

Currin, C. A., Chappell, W. S., Deaton, A., 2010. Developing alternative shoreline armoring strategies: The living shoreline approach in North Carolina. Proceedings of a State of the Science Workshop.

D'Andrea, A. F., Aller, R. C., Lopex, G. R., 2002. Organic matter flux and reactivity on a South Carolina sandflat: The impacts of porewater advection and macrobiological structures. Limnological Oceanography, 47 (4):1056-1070.

Davies-Vollum, K. S., West, M., 2015. Shoreline change and sea level rise at the Muni-Pomadze coastal wetland (Ramsar site), Ghana. Journal of Coastal Conservation 19:515-525.

De Swart, H.E., Zimmerman, J.T.F., 2009. Morphodynamics of Tidal Inlet Systems. Annual Review of Fluid Mechanics 41:203–229. doi:10.1146/annurev.fluid.010908.165159

Dean, W. E., 1974. Determination of carbonate and organic matter in calcareous sediments and sedimentary rocks by loss on ignition: comparison with other methods. Journal of Sedimentary Petrology 44:242-248.

Department of the Army/Corps of Engineers, Fiscal Years: 2012, 2011, 2010, 1998, 1997. Annual Reports of the Secretary of the Army on Civil Works Activities. Extract reports of the Wilmington, N.C., District.

Dillard, S. C., 2008. Resuspension events and seabed dynamics in the Neuse River Estuary, NC. MS Thesis, East Carolina University.

Dolan, R., Fenster, M. S., 1993. Historical shoreline trends along the Outer Banks, North Carolina: Processes and Responses. Journal of Coastal Research 9:172-188.

Douglass, S. L., Pickel, B. H., 1999. The tide doesn't go out anymore- The effect of bulkheads on urban bay shorelines. Shore and Beach 67:19-25.

Eulie, D. O., 2014. Examination of estuarine sediment dynamics: Insights from the large, shallow, Albemarle-Pamlico Estuarine System, NC, USA. Dissertation. East Carolina University, Coastal Resources Management.

Eulie, D. O., Walsh, J. P., Corbett, D. R., 2013. High-resolution analysis of shoreline change and application of balloon-based aerial photography, Albemarle-Pamlico Estuarine System, North Carolina, USA.

Feagin, R.A., Smith, W.K., Psuty, N.P., Young, D.R., Martínez, M.L., Carter, G.A., Lucas, K.L., Gibeaut, J.C., Gemma, J.N. and Koske, R.E., 2010. Barrier islands: coupling anthropogenic stability with ecological sustainability. *Journal of Coastal Research*, *26*(6), pp.987-992.

Findlay, S. E. G., Strayer, D. L., Smith, S. D., Curri, N., 2014. Magnitude and patterns of change in submerged aquatic vegetation of the tidal freshwater Hudson River. Estuaries and Coasts 37:1233-1242.

Fisher, John J. "Barrier island formation: discussion." Geological Society of America Bulletin 79.10 (1968)

Fourqurean, J. W., Duarte, C. M., Kennedy, H., Marbà, N., Holmer, M., Mateo, M. A., & Serrano, O., 2012. Seagrass ecosystems as a globally significant carbon stock. Nature Geoscience, 5(7):505-509.

Friedrichs, C. T., 2011. "3.06-Tidal Flat Morphodynamics: A Synthesis." Treatise on Estuarine and Coastal Science, edited by E. Wolanski and D. McLusky: 137-170.

Fugate, D. C., Friedrichs, C. T., 2002. Determining concentration and fall velocity of estuarine particle populations using ADV, OBS, and LISST. Continental Shelf Research, 22:1867-1886.

Gartner, J. W., 2004. Estimating suspended solids concentrations from backscatter intensity measured by acoustic Doppler current profiler in San Francisco Bay, California. Marine Geology 211:169-187.

Geis, S., Bendell, B., 2010. Charting the estuarine environment: A methodology spatially delineating a contiguous, estuarine shoreline of North Carolina. North Carolina Department of the Environment and Natural Resources, Division of Coastal Management.

Gittman, R.K., Popowich, A.M., Bruno, J.F., Peterson, C.H., 2014. Marshes with and without sills protect estuarine shorelines from erosion better than bulkheads during a Category 1 hurricane. Ocean & Coastal Management 102:94–102. doi:10.1016/j.ocecoaman.2014.09.016

Grabowski, R. C., Droppo, I. G., Wharton, G., 2011. Erodibility of cohesive sediment: The importance of sediment properties. Earth-Science Reviews 105:101-120.

Greiner, J. T., McGlathery, K. J., Gunnell, J., McKee, B. A., 2013. Seagrass restoration enhances "blue carbon" sequestration in coastal waters. PLoS ONE 8(8): e72469. doi:10.1371/journal.pone.0072469

GSAA, 1949 and 1974 Dare County Shoreline. Governors' South Atlantic Alliance. Unpublished data.

Hale, R. P., Ogston, A. S., Walsh, J. P., Orpin, A. R., 2014. Sediment transport and event deposition on the Waipaoa River Shelf, New Zealand. Continental Shelf Research 86:52-65.

Hall, M. O., Durako, M. J., Fourqurean, J. W., Zieman, J. C., 1999. Decadal changes in seagrass distribution and abundance in Florida Bay. Estuaries 22:445-459.

Hardin, E., Mitasova, H., Overton, M., 2012. GIS-Based analysis of storm vulnerability change at Pea Island, NC. Coastal Engineering, 2012.

Hawkins, D. W., 2015. Modern sedimentation and estuarine shoreline change around Roanoke Island, North Carolina. MS Thesis, East Carolina University.

Heiri, O., Lotter, A. F., Lemcke, G., 2001. Loss on ignition as a method for estimating organic and carbonate content in sediments: reproducibility and comparability of results. Journal of Paleolimnology 25:101-110.

Huettel, M., Rusch, A., 2000. Transport and degradation of phytoplankton in permeable sediment. Limnological Oceanography 45 (3):534-549.

Jackson, C. W., Alexander, C. R., Bush, D. M., 2012. Application of the AMBUR R package for spatio-temporal analysis of shoreline change: Jekyll Island, Georgia, USA. Computers & Geosciences 41:199-207.

Jackson, C. W., Alexander, C. R., Bush, D. M., 2012. Application of the AMBUR R package for spatio-temporal analysis of shoreline change: Jekyll Island, Georgia, USA. Computers & Geosciences 41:199-207.

Jackson, C.W., Jr., 2010. Basic User Guide for the AMBUR package for R, version 1.0a. Unpublished.

Jackson, N. L., Nordstrom, K. F., Eliot, I., Masselink, G., 2002. 'Low energy' sandy beaches in marine and estuarine environments: a review. Geomorphology 48:147-162.

Kelley, J. T., Pilkey, O. H., Cooper, J. A. G., 2009. America's most vulnerable coastal communities. Geological Survey of America Special Paper 460, 2009.

Kennedy, H., Beggins, J., Duarte, C. M., Fourqurean, J. W., Holmer, M., Marba, N., Middelburg, J. J., 2010. Seagrass sediments as a global carbon sink: Isotopic constraints. Global Biogeochemical Cycles 24.

Koch, E., 2001. Beyond light: Physical, geological, and geochemical parameters as possible submersed aquatic vegetation habitat requirements. Estuaries 24:1–17. doi:10.2307/1352808

Liu, J.T., Stauble, D.K., Giese, G.S., Aubrey, D.G., 1993. Morphodynamic Evolution of a Newly Formed Tidal Inlet, in: Formation and Evolution of Multiple Tidal Inlets. American Geophysical Union, pp. 62–94.

Luettich, R. A., Carr, S. D., Reynolds-Fleming, J. V., Fulcher, C. W., McNinch, J. E., 2002. Semi-diurnal seiching in a shallow, micro-tidal lagoonal estuary. Continental Shelf Research 22:1668-1681.

Mallinson, D. J., Smith, C. W., Culver, S. J., Riggs, S. R., Ames, D., 2010. Geological characteristics and spatial distribution of paleo-inlet channels beneath the outer banks barrier islands, North Carolina, USA. Estuarine, Coastal and Shelf Science 88:175-189.

Mallinson, D.J., Smith, C.W., Mahan, S., Culver, S.J., McDowell, K., 2011. Barrier island response to late Holocene climate events, North Carolina, USA. Quaternary Research 76:46–57. doi:10.1016/j yqres.2011.05.001

Mason, M. A., 2010. The transformation of waves in shallow water. Coastal Engineering Proceedings 1.1, 3.

Matias, A., Ferreira, Ó., Vila-Concejo, A., Garcia, T., Dias, J.A., 2008. Classification of washover dynamics in barrier islands. Geomorphology 97:655–674. doi:10.1016/j.geomorph.2007.09.010

Mcleod, E., Chmura, G. L, Bouillon, S., Salm, R., Bjork, M., Duarte, C. M., Lovelock, C. E., Schlesinger, W. H., Silliman, B. R., 2011. A blueprint for blue carbon: toward an improved understanding of the role of vegetated coastal habitats in sequestering CO_2. Frontiers in Ecology and the Environment 9(10):552-560.

McNinch, J., et al. (2012). "Observations of wave run-up, shoreline hotspot erosion, and sound-side seiching during Hurricane Irene at the Field Research Facility." Shore Beach, 80(2):19–37

Meyer, D. L., Townsend, E. D., Thayer, G. W., 1997. Stabilization and erosion control value of oyster cultch for intertidal marsh. Restoration Ecology 5:93-99.

Mulligan, R. P., Walsh, J. P., Wadman, H. M., 2014. Storm surge and surface waves in a shallow lagoonal estuary during the crossing of a hurricane. American Society of Civil Engineers.

National Hurricane Center, 2015. Hurricane Tracks at 2015. http://www.nhc.noaa.gov/data/tracks/tracks-at-2015.png

National Research Council, 2007. Mitigating Shore Erosion along Sheltered Coasts. Washington, US: National Academies Press. ProQuest ebrary. Web.

NC DCM, 2007 (Data). North Carolina's 2007 Estuarine Shoreline. Estuarine Shoreline Mapping Project. http://deq.nc.gov/about/divisions/coastal-management/coastal-management-data/spatial-data-maps

NC DCM, 2012 (Data). North Carolina's 2012 Estuarine Shoreline. Estuarine Shoreline Mapping Project.

NCDEQ, 2013. Weighing your options. How to protect your property from shoreline erosion: A handbook for estuarine property owners in North Carolina. Updated by the NC Division of Coastal Management – North Carolina Coastal Reserve & National Estuarine Research Reserve (NCNERR). http://portal.ncdenr.org/c/document_library/get_file?uuid=3ea68378-6f3f-4eb8-bd9d-04f6995f1d24&groupId=61572

O'Meara, T., Thompson, S. P., Piehler, M. F., 2015. Effects of shoreline hardening on nitrogen processing in estuarine marshes of the U.S. mid-Atlantic coast. Wetlands Ecology and Management 23:385-394.

Orth, R. J., Wilcox, D. J., Whiting, J. R., Kenne, A. K., Nagey, L., Smith, E. R., 2014. 2014 Distribution of submerged aquatic vegetation in Chesapeake Bay and coastal bays. Special Scientific Report #158. Virginia Institute of Marine Science.

Palinkas, C.; Koch, E., 2012. Sediment Accumulation Rates and Submersed Aquatic Vegetation (SAV) Distributions in the Mesohaline Chesapeake Bay, USA. Estuaries and Coasts 35:1416-1431.

Paphitas, D., Collins, M. B., 2005. Sediment resuspension events within the (microtidal) coastal waters of Thermaikos Gulf, northern Greece. Continental Shelf Research 25:2350-2365.

Peek, K.M., Mallinson, D.J., Culver, S.J., Mahan, S.A., 2013. Holocene Geologic Development of the Cape Hatteras Region, Outer Banks, North Carolina, USA. Journal of Coastal Research 30:41–58.

Peterson, C.H., Luettich, R.A., Micheli, F., Skilleter, G.A., 2004. Attenuation of water flow inside seagrass canopies of differing structure. Marine Ecology Progress Series 268.

Phillips, J.D., 1999. Event timing and sequence in coastal shoreline erosion: Hurricanes Bertha and Fran and the Neuse estuary. Journal of coastal research 616–623.

Pinsky, M. L., G. Guannel, and K. K. Arkema. 2013. Quantifying wave attenuation to inform coastal habitat conservation. Ecosphere 4(8):95. http://dx.doi.org/10.1890/ES13-00080.1

Pope, N. D., Widdows, J., Brinsley, M. D., 2006. Estimation of bed shear stress using the turbulent kinetic energy approach- A comparison of annular flume and field data. Continental Shelf Research 26:959-970.

Powell, M.A., Thieke, R.J., Mehta, A.J., 2006. Morphodynamic relationships for ebb and flood delta volumes at Florida's tidal entrances. Ocean Dynamics 56:295–307. doi:10.1007/s10236-006-0064-3

Powers, S. P., Peterson, C. H., Grabowski, J. H., Lenihan, H. S., 2009. Success of constructed oyster reefs in no-harvest sanctuaries: implications for restoration. Marine Ecology Progress Series 389:159-170.

Reed, D.J., D.A. Bishara, D.R. Cahoon, J. Donnelly, M. Kearney, A.S. Kolker, L.L. Leonard, R.A. Orson, and J.C. Stevenson. 2008. Site-Specific Scenarios for Wetlands Accretion as Sea Level Rises in the Mid-Atlantic Region. Section 2.1 in: Background Documents Supporting Climate Change Science Program Synthesis and Assessment Product 4.1, J.G. Titus and E.M. Strange (eds.). EPA 430R07004. U.S. EPA, Washington, DC.

Reynolds-Fleming, J. V., Luettich, R. A., 2004. Wind-driven lateral variability in a partially mixed estuary. Estuarine, Coastal and Shelf Science 60:395-407.

Reynolds-Fleming, J. V., Luettich, R. A., Fleming, J. G., 2013. Comparative hydrodynamics during events along a barrier island: explanation for overwash. Estuaries and Coasts 36:334-346.

Riggs, S. R., 2001. Shoreline erosion in North Carolina estuaries. 1-11 Vol. Raleigh, NC: North Carolina Sea Grant, NC State University.

Riggs, S. R., Ames, D. V., 2003. Book: Drowning NC Coast.

Riggs, S. R., Ames, D. V., Culver, S. J., Mallinson, D. J., Corbett, D. R., Walsh, J. P., 2009. Eye of a human hurricane: Pea Island, Oregon Inlet and Bodie Island, northern Outer Banks, North Carolina.

Riggs, S. R., Cleary, W. J., Snyder, S. W., 1995. Influence of inherited geologic framework on barrier shoreface morphology and dynamics. Marine Geology 126:213-234.

Riggs, S.R., Ames, D.V., Culver, S.J., Mallinson, D.J., 2011. The battle for North Carolina's coast: Evolutionary history, present crisis, and vision for the future. The University of North Carolina Press. Chapel Hill, NC, 160 pp.

Rusus, E., Soares, C. G., 2010. Validation of two wave and nearshore current models. Journal of Waterway Port Coastal and Engineering, January, 2010.

Scyphers, S. B., Powers, S. P., Heck, K. L., Byron, D., 2011. Oyster reefs as natural breakwaters mitigate shoreline loss and facilitate fisheries. PLoS ONE 6, Iss. 8.

Shepard, C. C., Crain, C. M., Beck, M. W., 2011. The protective role of coastal marshes: a systematic review and meta-analysis. Plos One 6, 11: e27374. doi:10.1371/journal.pone.0027374

Smith, Christopher G., Stephen J. Culver, Stanley R. Riggs, Dorothea Ames, D. Reide Corbett, David J. Mallinson, 2008. Geospatial analysis of barrier island width of two segments of the Outer Banks, NC, USA, anthropogenic curtailment of natural selfsustaining processes. Journal of Coastal Research 24, 70 pp.

Smith, K., North, E. W., Shi, F. Y., Koch, E. W., 2009. Modeling the effects of oyster reefs and breakwaters on seagrass growth. Estuaries and Coasts 32:748-757.

Soulsby, R. L., Humphery, J. D., 1990. Field observations of wave-current interaction at the sea bed. Book: Water Wave Kinematics, 413-428. Kluwer Academic Publishers.

Soulsby, R.L., 1983. The bottom boundary layer of shelf seas. *Elsevier oceanography series 35*:189-266.

Stick, David. The Outer Banks of North Carolina, 1584-1958. The University of North Carolina Press, 1958.

Stone, G.W., Liu, B., Pepper, D.A., Wang, P., 2004. The importance of extratropical and tropical cyclones on the short-term evolution of barrier islands along the northern Gulf of Mexico, USA. Marine Geology 210:63–78. doi:10.1016/j.margeo.2004.05.021

Strand, J., 2015. Examining coastal marsh sedimentation in the northeastern North Carolina. MS Thesis, East Carolina University.

Stutz, M. L., Pilkey, O. H., 2001. A review of global barrier island distribution. Journal of Coastal Research 34:15-22.

Swerida, R.M., 2013. Water flow and sediment grain size as co-varying SAV habitat requirements (M.S.). University of Maryland, College Park, Ann Arbor.

Timmons, E.A., Rodriguez, A.B., Mattheus, C.R., DeWitt, R., 2010. Transition of a regressive to a transgressive barrier island due to back-barrier erosion, increased storminess, and low sediment supply: Bogue Banks, North Carolina, USA. Marine Geology 278:100–114. doi:10.1016/j.margeo.2010.09.006

Tully, L. C., 2004. Evaluation of sediment dynamics using geochemical tracers in the Pamlico Sound Estuarine System, North Carolina. MS Thesis, East Carolina University.

U.S. Geological Survey, 2008. Critical shear stresses by particle-size classification for determining approximate condition for sediment mobility at 20 degrees Celsius. Scientific Investigations Report 2008-5093. http://pubs.usgs.gov/sir/2008/5093/table7.html

Wells, J., Kim, S.-Y., 1989. Sedimentation in the Albemarle-Pamlico Lagoonal System: Synthesis and Hypothesis. Marine Geology 88:263–284.

Whipple, A. C., Luettich, R. A., Seim, H. E., 2006. Measurements of Reynolds stress in a wind-driven lagoonal estuary. Ocean Dynamics 56:169-185.

Wicks, E. C., Koch, E. W., O'Neil, J. M., Elliston, K., 2009. Effects of sediment organic content and the hydrodynamic conditions on the growth and distribution of Zostera marina. Marine Ecology Progress Series 378:71-80.

Woodshole, 2005. U. S. Geological Survey Open-File Report 2005-1001. http://woodshole.er.usgs.gov/openfile/of2005-1001/htmldocs/videos/dry_sieve/dry_sieve.htm

Wren, D. G., Barkdoll, B. D., Kuhnle, R. A., Derrow, R. W., 2000. Field techniques for suspended-sediment measurement. Journal of Hydaulic Engineering 126:97-104.

Wright, L. D., Prior, D. B., Hobbs, C. H., Byrne, R. J., Boon, J. D., Schaffner, L. C., Green, M. O., 1987. Estuarine, Coastal and Shelf Science 24:765-784.

Zaremba, N., Mallinson, D. J., Leorri, E., Culver, S., Riggs, S., Mulligan, R., Horsman, E., Mitra, S., 2016. Controls on the stratigraphic framework and paleoenvironmental change within a Holocene estuarine system: Pamlico Sound, North Carolina, USA, Marine Geology, Volume 379, 1 September 2016, Pages 109-123, ISSN 0025-3227, http://dx.doi.org/10.1016/j.margeo.2016.04.012.

Zeller, R.B., Weitzman, J.S., Abbett, M.E., Zarama, F.J., Fringer, O.B., Koseff, J.R., 2014. Improved parameterization of seagrass blade dynamics and wave attenuation based on numerical and laboratory experiments. Limnology and Oceanography 59:251–266. doi:10.4319/lo.2014.59.1.0251

Zhou, L., Liu, J., Saito, Y., Zhang, Z., Chu, H., Hu, G., 2014. Coastal erosion as a major sediment supplier to continental shelves: example from the abandoned Old Huanghe delta. Continental Shelf Research 82:43-59.

Appendix A: Region Shoreline Change Rates

Region	Year	Mean Change (m)	Mean Change Rate (m y^{-1})
1	1949-1974	-11.9 ± 3.5	-0.45 ± 0.1
	1974-2007	-11.2 ± 1.6	-0.34 ± 0.1
	2007-2012	-0.3 ± 1.6	-0.06 ± 0.3
	2012-2015	-3.3 ± 1.7	-0.92 ± 0.6
2	1949-1974	-11.5 ± 3.5	-0.46 ± 0.1
	1974-2007	-17.9 ± 1.6	-0.54 ± 0.1
	2007-2012	1.7 ± 1.6	0.35 ± 0.3
	2012-2015	-4.0 ± 1.7	-1.11 ± 0.6
3	1949-1974	3.0 ± 3.5	0.12 ± 0.1
	1974-2007	-19.4 ± 1.6	-0.59 ± 0.1
	2007-2012	-1.0 ± 1.6	-0.21 ± 0.3
	2012-2015	-5.1 ± 1.7	-1.35 ± 0.6
4	1949-1974	-26.5 ± 3.5	-1.06 ± 0.1
	1974-2007	-29.7 ± 1.6	-0.90 ± 0.1
	2007-2012	0.3 ± 1.6	0.07 ± 0.3
	2012-2015	-1.2 ± 1.7	-0.33 ± 0.6
5	1949-1974	-4.7 ± 3.5	-0.19 ± 0.1
	1974-2007	-7.2 ± 1.6	-0.22 ± 0.1
	2007-2012	0.2 ± 1.6	0.04 ± 0.3
	2012-2015	-3.0 ± 1.7	-0.84 ± 0.6

Appendix B: Percent Shoreline Type

Region	Shore Type	1949	1974	2007	2012	2015
1	Marsh	97.7	93.9	99.6	100.0	94.3
	Sed Bank	2.3	6.1	0.4	0.0	5.7
	Modified	0.0	0.0	0.0	0.0	0.0
2	Marsh	70.8	57.2	52.0	82.9	45.7
	Sed Bank	29.2	42.8	47.0	15.6	44.2
	Modified	0.0	0.0	1.0	1.5	10.1
3	Marsh	80.0	86.4	77.0	76.9	71.1
	Sed Bank	13.7	7.3	18.0	14.4	20.6
	Modified	6.4	6.4	5.0	8.7	8.3
4	Marsh	60.0	52.1	31.0	21.0	10.5
	Sed Bank	40.0	39.6	34.0	27.6	4.5
	Modified	0.0	8.3	35.0	51.5	85.0
5	Marsh	73.7	93.4	65.0	67.7	69.4
	Sed Bank	26.3	5.3	25.0	14.5	9.7
	Modified	0.0	1.3	10.0	17.8	20.9
All	Marsh	76.4	76.6	64.9	69.7	58.2
	Sed Bank	22.3	20.2	24.9	14.4	16.9
	Modified	1.3	3.2	10.2	15.9	24.9

Appendix C: Shoreline Volumetric Change Rates, 1949 - 2015

Region	Mean SCR ($m\ y^{-1}$)	Mean Scarp (m)	Shoreline (m)	VCR (m^3/y)		Baseline (m)	VCR (m^3/y)		ACR (m^2/y)	VCR (m3/y)
1	-0.38 ± 0.03	0.23 ± 0.02	9406	-800 ± 67		2867	-240 ± 67		-1400 ± 21	-320 ± 22
2	-0.48 ± 0.03	0.45 ± 0.02	1261	-270 ± 52		742	-160 ± 52		-371 ± 21	-170 ± 11
3	-0.34 ± 0.03	0.55 ± 0.02	3199	-600 ± 72		1113	-210 ± 72		-587 ± 21	-320 ± 9
5	-0.22 ± 0.03	0.47 ± 0.02	2320	-240 ± 110		1375	-150 ± 110		-345 ± 21	-160 ± 10
			Total	**-1910 ± 156**			**-760 ± 156**			**-970 ± 28**

Appendix D: Scarp Measurements

Scarp Heights (m)

Region	Mean Scarp	Scarp 1	Scarp 2	Scarp 3	Scarp 4	Scarp 5	Scarp 6	Scarp 7
1	0.23	0.14	0.29	0.18	0.21	0.26	0.41	0.10
2	0.45	0.47	0.55	0.40	0.47	0.35	N/D	N/D
3	0.55	0.51	0.58	0.59	0.63	0.46	0.87	N/D
5	0.47	0.43	0.41	0.34	0.58	0.65	0.60	0.30

N/D = No data

Scarp Sample LOI

Date	Region	Pre-ignition (g)	Post-ignition (g)	% LOI
22-Jun	1	2.25	1.68	25.5
22-Jun	2	3.05	2.73	10.6
22-Jun	3	4.36	4.08	6.5
22-Jun	5	1.73	1.38	20.3

Appendix E: Sediment Sample Results (µm)

Date	Sample ID	Mean	Sorting	Skewness	Kurtosis	d10	d50	d90
22-Jun	1	147	105	9.9	194	83	124	217
22-Jun	3	154	90	10.7	257	92	138	228
22-Jun	5	170	136	9.3	124	94	148	236
22-Jun	7	246	109	3.6	34	138	224	347
22-Jun	9	259	144	3.4	22	137	222	394
22-Jun	11	145	97	12.2	246	92	131	179
22-Jun	13	164	51	4.6	50	118	154	221
22-Jun	15	182	106	9.4	172	102	163	254
22-Jun	17	260	120	2.5	16	139	235	382
22-Jun	19	132	128	11.2	183	71	108	178
22-Jun	21	130	67	18.1	549	91	118	172
22-Jun	23	151	103	12.5	224	92	140	195
22-Jun	25	179	94	3.1	26	92	158	285
22-Jun	27	279	122	2.6	16	160	256	409
22-Jun	29	125	76	6.5	74	75	109	173
22-Jun	31	177	88	6.9	189	95	159	270
22-Jun	33	243	118	2.6	17	123	220	352
22-Jun	35	204	127	8.7	120	129	178	295
22-Jun	37	122	119	10.3	160	67	101	173
22-Jun	39	152	104	3.7	26	77	116	261
22-Jun	40	205	94	3.3	26	110	192	305
22-Jun	41	226	67	2.9	29	147	215	312
22-Jun	43	221	94	1.9	16	115	208	330
22-Jun	44	221	93	4.2	44	132	206	318
22-Jun	45	281	156	3.5	25	142	251	431
22-Jun	47	205	128	3.5	31	80	184	329
22-Jun	49	206	131	8.7	117	113	190	291
22-Jun	51	142	107	12.5	217	83	128	181
22-Jun	53	175	153	7.9	89	81	150	261

22-Jun	55	231	118	3.2	24	127	207	343
22-Jun	57	195	137	7.7	97	97	172	292
22-Jun	59	195	60	3.6	41	129	190	247
22-Jun	61	223	91	2.4	20	122	210	325
22-Jun	63	229	118	3.9	38	119	210	339
22-Jun	65	250	117	3.7	31	136	229	346
22-Jun	67	204	97	6.4	140	113	187	306
22-Jun	69	179	111	10.2	165	101	161	244
22-Jun	71	203	99	5.3	71	106	192	306
22-Jun	73	231	104	4.1	34	138	211	324
22-Jun	75	231	136	4.6	37	130	200	335
22-Jun	77	226	101	9.1	173	135	213	318
22-Jun	79	187	100	6.4	83	96	176	274
22-Jun	81	284	139	3.6	26	158	259	403
22-Jun	C2	178	115	7.5	118	82	157	289
22-Jun	C3	227	110	3.6	33	117	209	333
16-Dec	1	157	99	6.4	71	93	133	234
16-Dec	7	243	112	3.5	29	136	221	347
16-Dec	13	160	62	8.3	114	110	150	209
16-Dec	26	265	110	3.2	27	158	240	374
16-Dec	33	242	125	3.6	31	125	218	352
16-Dec	39	156	127	8.5	169	73	117	273
16-Dec	41	213	128	9.4	129	128	199	293
16-Dec	43	219	96	3.0	26	120	205	324
16-Dec	45	262	184	6.2	71	127	226	402
16-Dec	50	197	66	5.5	71	132	188	249
16-Dec	55	181	93	4.3	42	93	165	264
16-Dec	59	178	73	7.6	103	126	163	237
16-Dec	61	236	108	3.2	28	123	218	341
16-Dec	63	225	118	3.8	37	109	206	339
16-Dec	75	205	108	5.2	51	119	185	301
16-Dec	79	196	93	6.0	80	109	186	282

Appendix F: Loss on Ignition Results

Date	ID	Pre-ignition (g)	Post-ignition (g)	% LOI
22-Jun	1	5.7512	5.7189	0.56
22-Jun	3	7.1539	7.1109	0.60
22-Jun	5	6.1972	6.1378	0.96
22-Jun	7	8.5017	8.4563	0.53
22-Jun	9	8.9945	8.9523	0.47
22-Jun	11	9.7693	9.7129	0.58
22-Jun	13	8.4944	8.4550	0.46
22-Jun	15	7.1562	7.0998	0.79
22-Jun	17	7.8147	7.7753	0.50
22-Jun	19	7.9006	7.8468	0.68
22-Jun	21	9.5521	9.4938	0.61
22-Jun	23	8.7615	8.6852	0.87
22-Jun	25	10.1830	10.1113	0.70
22-Jun	27	9.5344	9.4978	0.38
22-Jun	29	11.3475	11.2653	0.72
22-Jun	31	10.9043	10.8532	0.47
22-Jun	33	8.2096	8.1716	0.46
22-Jun	35	7.3780	7.3222	0.76
22-Jun	37	9.8299	9.7342	0.97
22-Jun	39	8.0160	7.9666	0.62
22-Jun	40	9.9869	9.9476	0.39
22-Jun	41	10.1810	10.1438	0.37
22-Jun	43	8.8923	8.8421	0.56
22-Jun	44	9.2939	9.2516	0.46
22-Jun	45	8.7943	8.7251	0.79
22-Jun	47	11.8300	11.7661	0.54
22-Jun	49	8.2532	8.2130	0.49
22-Jun	51	8.4577	8.4026	0.65
22-Jun	53	9.6815	9.5473	1.39
22-Jun	55	10.5006	10.4650	0.34

22-Jun	57	7.4722	7.4289	0.58
22-Jun	59	6.4032	6.3819	0.33
22-Jun	61	8.058	8.0285	0.37
22-Jun	63	7.9594	7.8995	0.75
22-Jun	65	7.9303	7.9056	0.31
22-Jun	67	7.5928	7.5643	0.38
22-Jun	69	6.9582	6.9110	0.68
22-Jun	71	7.2933	7.2502	0.59
22-Jun	73	7.3197	7.2960	0.32
22-Jun	75	7.2668	7.2411	0.35
22-Jun	77	7.4832	7.4638	0.26
22-Jun	79	7.1148	7.0730	0.59
22-Jun	81	8.4949	8.4686	0.31
16-Dec	1	22.7905	22.7369	0.24
16-Dec	7	21.7169	21.6552	0.28
16-Dec	13	21.6057	21.5693	0.17
16-Dec	26	25.1887	25.1523	0.14
16-Dec	33	22.9151	22.8714	0.19
16-Dec	39	22.5183	22.4448	0.33
16-Dec	41	23.1040	23.0583	0.20
16-Dec	43	26.6402	26.5774	0.24
16-Dec	45	22.0408	21.9124	0.58
16-Dec	50	23.1413	23.1050	0.16
16-Dec	55	21.1060	21.0610	0.21
16-Dec	59	21.3704	21.3365	0.16
16-Dec	61	23.7266	23.6786	0.20
16-Dec	63	21.1713	21.0845	0.41
16-Dec	75	23.0216	22.9785	0.19
16-Dec	79	26.6142	26.5555	0.22